THESIS

EXPERIMENTAL INVESTIGATIONS FOR IMPROVING THE ACCURACY OF FLOW MEASUREMENT IN IRRIGATION CANALS

Submitted by

Joseph E. Pugh

Department of Civil and Environmental Engineering

In partial fulfillment of the requirements

For the Degree of Master of Science

Colorado State University

Fort Collins, Colorado

Summer 2021

Master's Committee:

Advisor: S. Karan Venayagamoorthy
Co-Advisor: Timothy K. Gates

Bret C. Windom

ABSTRACT

EXPERIMENTAL INVESTIGATIONS FOR IMPROVING THE ACCURACY OF FLOW MEASUREMENT IN IRRIGATION CANALS

Flow measurement in open-channels refers to the process by which a volume amount of water passing through a channel cross section is quantified per unit time. In the irrigation water management context, this is done to account for available water resources so that water distribution systems can be properly managed to achieve adequate and efficient allocation. Today, irrigation water use remains the largest consumptive draw on our collective water budget, while the availability of this resource is becoming increasingly scarce. Additionally, access to reliable irrigation water acts as a major factor in maintaining strong crop production and healthy rural livelihoods. Improvement in the accuracy of flow measurement methodologies is then motivated by a need for implementing more conservative practices to limit unnecessary waste and to promote effective and equitable allocation.

The two principal means by which flow is quantified in open-channels are: the velocity-area (section-by-section) method, and the use of stage-discharge relationships associated with hydraulic structures placed within the channels. The present study investigates improvements to the accuracy of flow measurement for each of these methodologies.

The velocity-area method involves the integration of several point measurements of velocity multiplied by sub-components of the channel cross-sectional area to achieve an estimate of flow rate via the principle of continuity. Traditionally, these methods have been time-consuming and subject to inaccuracy due to the large number of measurements needed. In recent decades, the development of Acoustic Doppler Current Profilers (ADCPs) has offered a means for measuring flow using the velocity-area method with time-efficiency and less intrusiveness into the flow. However, opportunity still exists for refining the operational protocols for this device to quantify and reduce

measurement uncertainty, especially within the irrigation water management context. With this motivation, a *StreamPro* ADCP manufactured by *Teledyne RD Instruments* was used to quantify flow rates in artificially-constructed irrigation canals with the aim of determining best practices for: the method of deployment of an ADCP using a moving boat, the duration of the measurement transect per unit width of canal, and the number of transects to use in computing mean steady discharge. The purpose of these refinements is to better resolve a mean representation of the fluctuating turbulent velocity flow field by lessening user-induced uncertainty and estimating the point of diminishing returns for additional data collection. Suggested protocols developed from this experimentation indicate that a reduction of 30 to 70% in the values of uncertainty metrics can be accomplished utilizing a remotely operated tagline deployment method with a minimum transect duration relative to the canal top width of 24 s/m (7.3 s/ft), equivalent to 24 vertical pings per meter of an ADCP measuring at 1 Hz; and at least six total transects taken in reciprocal directions included in measurements of mean steady discharge. These findings provide further specificity beyond current guidelines to enhance the likelihood of practical implementation by ADCP users.

Refinement of ADCP measurement protocols also serves as a chief aid in the accuracy of hydraulic structure calibration. As permanent fixtures within an open-channel, these structures represent a means of obtaining continuous flow measurement without the time cost of velocity-area methods. The fundamental principle upon which hydraulic structures operate is the stage-discharge relationship. This equation relates an upstream measurement of the water surface elevation to the flow rate passing through the channel. However, the theoretical derivation of stage-discharge equations require several simplifying assumptions that must be corrected for using empirical calibration.

In the present study, the nature of the stage-discharge relationship for a particular hydraulic structure known as the Obermeyer pivot weir is investigated. This device was primarily designed as a control for upstream water levels, and the current effort to establish a means by which the weir can be used for flow measurement purposes represents a novel contribution to the literature. In general, research on pivot weirs remains sparse, and no consensus has been reached concern-

ing the correct theoretical approach for establishing the stage-discharge equation for this type of structure. Here, using a set of field observations, four alternative approaches are investigated to elucidate the optimal method for the use of pivot weirs for flow measurement. Specifically, a hypothesis concerning the effect of the changing angle of a pivot weir on the flow dynamics is tested. A recommended approach is given and informed by knowledge of practical implementation limitations. Finally, preliminary investigations using a laboratory model of the Obermeyer pivot weir are discussed, which offer insight into the complex nature of the dynamics for flow over this type of structure. The results of the present study offer important refinements to the current body of knowledge found within the literature and identify promising avenues for future research.

ACKNOWLEDGEMENTS

The completion of this M.S. thesis has primarily been a testament to the grace and encouragement shown to me by others along the way. First, I express my sincere gratitude and appreciation for the guidance and opportunities for growth provided to me by my advisor, Dr. S. Karan Venayagamoorthy. I came to CSU as a very "green" post-graduate with a B.A. in Biology and a dream to become an engineer. Dr. Karan saw some potential in me as a student in his undergraduate fluid mechanics course and took a chance on me as a research student in the Environmental Fluid Mechanics Laboratory. This decision has allowed me to blossom as a practical experimentalist and kindled within me a passion for studying fluid dynamics. Thank you Dr. Karan for your support of my studies, your words of wisdom, and your passion for education. They have truly been an inspiration to me. Additionally, I would like to thank my co-advisor Dr. Timothy K. Gates for his enduring support, stimulating conversations, and commitment to conducting research with a high level of integrity. His guidance in this thesis project has been invaluable; allowing me to improve my scientific writing skills immensely and fortifying my intellectual understanding of the topics at hand. Thank you both, Dr. Karan and Dr. Gates.

I also wish to thank:

- The Colorado Agricultural Experiment Station for funding this work. (grant no. COL00788)

- My peers in the Environmental and Fluid Mechanics Laboratory for their inspiration and camaraderie these past two years. Jessica Baker, Joey Sinclair, Harshit, Matthew Klema, Dr. Oladapo Aseperi, and Daniel Sanchez - thank you. I could not have imagined taking on this project as solitary pursuit without your willingness to candidly discuss an aspect of research or simply enjoy a conversation as friends.

- My friends within the Civil and Environmental Engineering Program at CSU; and Environmental and Water Resources Institute: Most especially, BJ Elkins and Ben Irvin, for your companionship and willingness to invest in the culture of the program and pursue enriching experiences during our time at CSU.

- Andy Pineda, Kyle Johnson, and Jeff Schott of the Larimer and Weld Irrigation company for their assistance in conducting field work and education on irrigation system dynamics.
- Joey Sinclair, Rehman Lund, Harshit, and Josh McMartin - specifically for their contributions in collecting field observations and good humor even in uncomfortable conditions when something inevitably went awry with our measurements!
- My family: Mom, Dad, Tom, Madeline, and Mary Cate; for their unwavering support, prayers, inspiration, and willingness to debrief with me over our weekly calls concerning the ups and downs of graduate studies.
- Justin Van Ee and Austin Cassel, my roommates for the majority of my studies; for their support of and interest in my research, fellowship in Christ, and many enjoyable game nights.
- My friends at Iasis Christ Fellowship in Fort Collins for their love, prayers, and edification. Specifically to Luke Worden, Jake Leohr, and Chun Lee for their discipleship and close companionship.

Lastly I thank my gracious Savior and Redeemer, my source of comfort through all manner of trials, Jesus Christ. His ever-near presence and willingness to constantly intercede on my behalf has been my sustaining strength through these studies. Ultimately, I am thankful for this beautiful created order that has been imbued with His glory and that I am fortunate to study with the abilities He has granted me.

TABLE OF CONTENTS

LIST OF TABLES

LIST OF FIGURES

Chapter 1

Introduction

1.1 Background and Motivation

Although using water for irrigating agricultural land may be an inconspicuous process to most, on a global scale it has historically been the largest demand on our collective water supply and served as a major catalyst for development [1,2]. Growing populations require food, and in areas of either sparse precipitation or dense populations, irrigation is necessary to support society. This requirement brings with it the need for transporting and allocating water from a supply source, such as a river or reservoir, to agricultural land which may be several miles downstream. Conveyance of irrigation water is achieved through the use of engineered canals - a type of open-channel that is narrower and deeper than a natural stream, but where the flow is still driven by gravity.

The process of regulating and quantifying the flow of water within irrigation canals is achieved through the use of hydraulic structures. Broadly, these structures can be weirs (i.e. small dams), spillways, gates, or even specialized flumes. The primary purpose of hydraulic structures operating within open-channels is to control the flow conditions within the channel, and secondarily to quantify the volume amount of water passing through the channel at a given time. These two broad purposes can be defined succinctly as flow regulation and measurement.

The goal of accurately measuring the volume of water moving through an open-channel contributes to the main system objectives for an irrigation water delivery network: delivering an adequate volume of water, efficiently conserving water through loss reduction, achieving dependability in the timing and amount of the delivery, and maintaining equity in that the delivered amount is fair to the particular right of the user [3]. In areas where irrigation is necessary, water is a highly coveted scarce resource. In many cases, such as in the Western U.S., legal codes exist which allow private users to claim water as their own property to be used as a means for economic production. The high premium of water in these cases creates the need for distribution systems that do not waste water, where users receive a proportionate amount of water for which they have a right, and that the water is delivered in a timely and dependable manner. This goal has social and environmental justice implications as well. Historically, upstream water users have sometimes enjoyed the privilege of unrestricted access over downstream users when accurate flow quantification was not prioritized [4]. Additionally, uncertainty in flow measurement increases the difficulty for system managers to properly budget and track where water is stored and where it is being used. Thus, increasing the accuracy and reliability of flow measurement within irrigation systems promotes robust decision making and reduces economic costs [5].

Furthermore, increased motivation for improving the accuracy of flow quantification methods within irrigation systems is found in the mounting pressure that a warming climate and population growth are placing on our systems. Into the future, higher populations will drive food production systems to become more efficient while operating on less acreage due to urbanization. This in turn will require that the irrigation systems that supply the water necessary for food production also respond with more accurate allocation and less operational costs. Finally, warming temperatures may increase evapotranspiration rates of crops, while also contributing to less predictability in precipitation patterns [6]. These combined effects put further stress on irrigation systems and motivate the effort to enhance the accuracy of flow quantification.

The basic mechanism for quantifying flow rate through open-channels is the stage-discharge (rating) relationship. This is a mathematical equation that relates the "head", or energy per unit weight of flowing water, upstream of a hydraulic structure to an estimated discharge value that passes through the structure (see Figure 1.1). These equations are semi-empirical in nature, in that they operate under some assumption of critical or potential (inviscid) flow, while allowing for the incorporation of a corrective discharge coefficient that requires calibration and is dependent on the design geometry of the structure. The calibration process for a hydraulic structure is achieved through the use of an independent measurement of flow rate that is paired with associated measurements of the head level upstream of the structure. An increasingly popular method for achieving this independent discharge measurement is through the use of acoustic Doppler techniques, which

Figure 1.1: An Obermeyer pivot weir in an irrigation canal in Weld County, Colorado as an example of a hydraulic structure operating as flow measurement and regulation device. View is upstream.

are discussed in depth later on. This process allows for determining the empirical discharge coefficient that should be used for a specific structure under a range of operational guidelines.

Some common structures used within irrigation canals for measurement and regulation are weirs (sharp-crested, broad-crested, pivot, or otherwise), sluice gates, and Parshall flumes. If a head-discharge relationship is available, canal managers can then use a simple measurement of water surface elevation upstream of the structure to gain an estimate of flow rate within the canal.

1.2 Objectives

The task of accurate flow quantification for the purpose of sound irrigation water management requires reliable calibration of measurement structures and a firm theoretical understanding of the governing principles that are incorporated into a head-discharge relationship. The primary goal of this thesis research is to enhance the accuracy of flow measurement methods within irrigation canals through experimental investigations of hydraulic structures under operational conditions, as well as observing and analyzing flow over scaled laboratory models. This is addressed primarily through two objectives.

The first objective is the refinement of protocols for measurements made using an acoustic Doppler current profiler (ADCP) to reduce the uncertainty in discharge quantification. This work allows hydraulic structures to be calibrated more accurately using ADCPs and enhances the ability for improvement of auxiliary elements of irrigation water management, such as quantifying seepage losses [7].

The second objective of this thesis is to describe the nature of the stage-discharge relationship for a specific type of hydraulic structure known as an Obermeyer pivot weir. Currently, this structure is primarily used simply as a regulating device to control upstream water levels; the development of a rating equation for this type of structure is an area of emerging research.

1.3 Thesis Layout

This thesis contains an additional four chapters. In the succeeding chapter, a literature review is presented concerning the topics of irrigation water measurement and management, discharge quantification using an ADCP, and the design principles and rating equation theory for an Obermeyer pivot weir. Chapter Three presents the draft of a manuscript that has been submitted for publication concerning the refinement measurement protocols to reduce uncertainty in ADCP discharge measurement. Chapter Four presents results of field observation and preliminary laboratory findings to discuss several aspects of consideration for developing a head-discharge rating equation for the Obermeyer pivot weir. Chapter Five concludes with a summary of relevant findings and a description of avenues for future research.

Chapter 2

Literature Review of Flow Quantification in open-channels

The task of flow measurement may not seem an illustrious endeavor, but its importance to human society has been monumental. This process is necessary for efficiently allocating resources, namely water, as well as monitoring the environment to prevent environmental hazards such as floods. Throughout early history, applications of flow measurement techniques can be found in the reservoir construction and flood management techniques of the Chinese, the irrigation networks of the Egyptians, and the aqueducts constructed to convey water by the Romans. Each of these feats of ancient hydraulic engineering required some rudimentary knowledge of flow measurement that allowed human civilization to flourish [8]. Since then, the Scientific Revolution and advent of classical fluid mechanics has allowed for the furtherance of our ability to measure flow through open-channels. Now that the basic exercise of flow measurement is a possibility (and has been for some time), the question now turns to ways of measuring flow in open-channels with the highest level of practical accuracy. In this chapter, a brief review of the governing equations for fluid flow are discussed, followed by a description of the main methods used for open-channel flow measurement. Lastly, the theoretical nature of the the stage-discharge rating equation for one specific hydraulic structure in particular - the pivot weir, is reviewed.

2.1 Governing Equations

The fundamental governing equations for fluid mechanics are the momentum (Navier-Stokes) equations. Assuming incompressible flow ($\nabla \cdot \mathbf{u} = 0$), these equations can be written in the Lagrangian perspective as:

$$\rho \frac{D\mathbf{u}}{Dt} = -\nabla P + \rho \mathbf{g} + \mu \nabla^2 \mathbf{u}. \tag{2.1}$$

Here, $\mathbf{g}$ is the gravitational acceleration constant acting in the vertical, (y), direction, and $\mathbf{u}$ is the three-dimensional velocity tensor. Equation (2.1) is an application of Newton's second law, and states that the advection of fluid momentum is determined by the interacting effects of pressure - P, buoyancy - ρg, and viscosity - μ.

As a special case, Eq. (2.1) can be reduced to the Euler equation for inviscid flows, where gravity becomes the only relevant body force. Then, the advective acceleration terms on the right side of Eq. (2.1) can be re-written in terms of the velocity-vorticity cross product summed with the gradient of the kinetic energy per unit mass. If irrotational (i.e. $\omega = 0$) and barotropic ($d\rho/dP = 0$) conditions are also assumed, then the Bernoulli equation for constant density, steady flow can be derived from Eqns. (2.1) and written as[1]:

$$\frac{1}{2}|\mathbf{u}|^2 + \frac{P}{\rho} + \mathbf{g}z = \text{constant along streamlines.} \tag{2.2}$$

Eq. (2.2) is commonly used in the field of fluid mechanics for applications in both closed conduit and open-channel flow where the flow is far removed from solid boundaries (wall). In these regions, viscous effects due to fluid friction along the wall may be safely ignored. The study of fluid flow without consideration of viscous effects is referred to as *potential* or *ideal* flow [9]. This is the simplest class of flows available for study in fluid mechanics, and several fundamental observations on the approximate nature of flow phenomena over solid bodies have been made using this set of simplifying assumptions. However, in practical engineering applications in open-channels the flow is far from being ideal in the sense that it is often highly turbulent. This turbulence violates the assumption of irrotational flow, especially near the wall where boundary layer separation occurs. Even so, the application of Eq. (2.2) and its implicit assumptions to practical flows in hydraulic engineering are still widely used today, albeit with the incorporation of empirical correction coefficients.

[1] see [9] for full derivation of Eq. (2.2)

The next governing equation for flow measurement in open-channels is the continuity, or conservation of mass, equation. From a control volume perspective, this equation can be written for one-dimensional open-channel flow as:

$$\frac{\partial Q}{\partial x} + \frac{\partial A}{\partial t} + q_l = 0. \tag{2.3}$$

Here, Q is the volumetric flowrate $[L^3/T]$, A is the cross-sectional area $[L^2]$ of the channel, and q_l is the lateral flux term per unit length $[L^2/T]$. Figure 2.1 provides reference for the coordinate system used for open-channel flow. x,y, and z are the principal Cartesian coordinate directions.

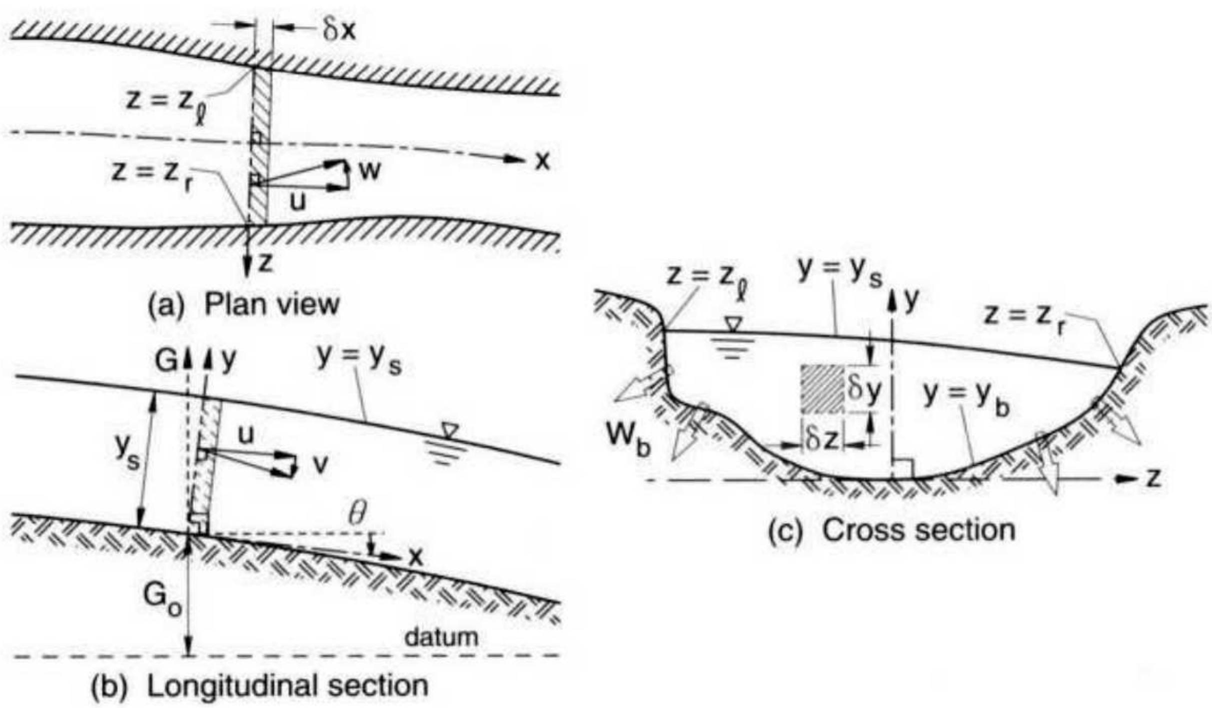

Figure 2.1: Illustration of the conventional coordinate system used for open-channel flows, from Jain 2001.

Here, x represents the stream-wise direction along the channel Thalweg axis (i.e. point of maximum depth). y and z are perpendicular to x and represent the depth-wise, and transverse flow directions, respectively. y_s is the location of the water surface elevation and y_b is the depth of the channel bed, with z_l and z_r representing the location of the left and right banks, respectively.

W_b is the weight the water exerts on the channel bed. u, v, and w are the components of the three-dimensional velocity tensor, associated respectively with the x, y, and z directions. G, or alternatively g, represents the gravitational acceleration force acting in the vertical.

The continuity equation for open-channel flow invokes the kinematic boundary condition for the free surface. When the flow is assumed steady and lateral flux contributions are neglected, Eq. (2.3) can be integrated and written as the familiar one-dimensional continuity equation for incompressible open-channel flow: $Q = \overline{U}A$. Here, $\overline{U}$ is the depth averaged stream-wise flow velocity in the channel. With knowledge of the channel geometry and means for measuring the flow velocity and water surface elevation, Eq. (2.3) allows for the computation of steady discharge within an open-channel.

2.2 Methods for open-channel Flow Measurement

2.2.1 Velocity-area method utilizing point velocity current meters

There are several methods by which computation of volumetric flow rate in an open-channel may be achieved. The most basic approach is known as the velocity-area method, by which several measurements of flow velocity are taken at vertical cross-sections within the channel. Discharge is then derived by integrating the products of velocity, depth, and distance between verticals. Flow velocity may be determined via a number of possible instruments, known as current meters. These instruments may be primarily mechanical in nature, such as the commonly-used propeller-type current meters which relate the speed of the water flow to the angular velocity of the rotating propeller. Alternatively, an Acoustic Doppler Velocimeter (ADV) may be used which emits pulse of sound waves into the water, which are then reflected back to the instrument by suspended sediment. The velocity of these sediment particles can then by determined using the principle of the Doppler effect.

Flow quantification via the velocity-area method using point-measurement current meters is relatively straightforward to implement due to the simple and reliable nature of the instrumentation [10]. However, for larger channels this method can be especially time consuming. Typically, this method is utilized to relate a measurement of the water stage at a gauging stage to the discharge computed so that a stage-discharge relationship can be established for the particular channel cross section. However, due to the time-intensive nature of the velocity-area method, uncertainty is introduced into the stage-discharge relationship when the flow rate becomes unsteady during the time of measurement. Unsteady flows in artificially constructed channels are less common than in natural streams, however consideration still must be given to the possibility of unsteady flow within the channel reach during the time of discharge measurement. For this reason, it is prudent to conduct the measurement in a manner that is as time-efficient as possible without sacrificing accuracy.

Figure 2.2: Flow rate quantification via the velocity-area method, utilizing an ADV. Figure 2.7c in [10].

Furthermore, the velocity-area method is often conducted in a way that is intrusive in to the flow. For channels that do not have a structure spanning the width of the measurement cross-section it is necessary for the hydrographer to wade into the stream with the current meter to conduct the measurement (see Figure 2.2). In the majority of measurement cross-sections the flow will be sub-critical, and as such any intrusive disturbance into the flow will be propagated both upstream and downstream. This disturbance is likely to change the nature of the surrounding flow, potentially biasing the velocity measurement. This represents a drawback of intrusive point velocity-area measurement.

2.2.2 Velocity-area method utilizing Acoustic Doppler Current Profiler

The Acoustic Doppler Current Profiler (ADCP), shown in Figure 2.3, represents an alternative method for determining discharge within an open-channel that mitigates some of the time and intrusiveness restraints of the aforementioned velocity-area method of point velocity measurement. In essence, the ADCP is a compact cylindrical probe that is typically mounted on a small boat,

Figure 2.3: A StreamPro ADCP measuring discharge within an irrigation canal in Larimer County, Colorado. Remotely-operated tagline deployment using the *ADCP Traveler* is also shown.

enabling it to move along a cross-section of the channel that is perpendicular to the direction of the flow. In principle, this instrument still estimates discharge via the velocity-area method. However, the ADCP represents a time-efficient method in its ability to simultaneously calculate the mean velocity of multiple "cells" within a vertical measurement ensemble along the depth of the channel (see Figure 2.4).

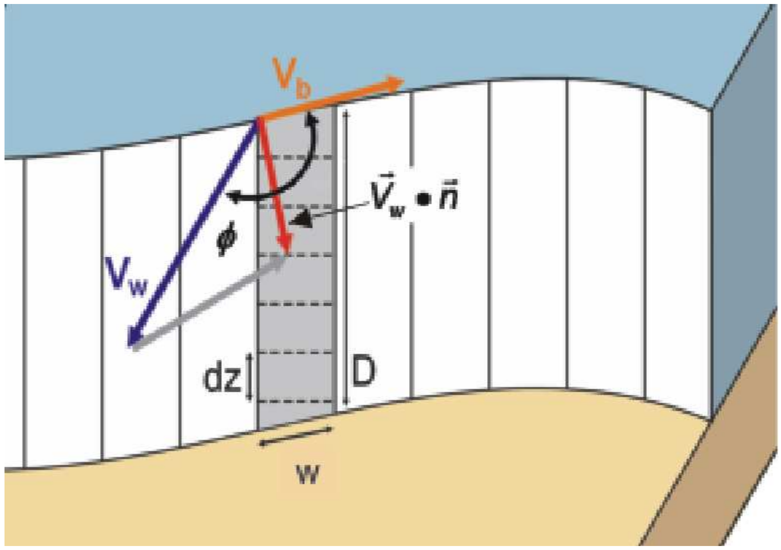

Figure 2.4: Representation of boat velocity, V_b, and water velocity V_w vectors for a single ADCP depth cell within a vertical measurement ensemble. dz is the differential cell depth, D is the ensemble depth, and w is the distance between vertical ensembles. Taken from Figure A-5 in [11].

The general mode of operation for the ADCP is to move from one bank of the channel to the other as smoothly as possible. As the ADCP travels along this channel cross-section, it sends out acoustic "pings" downward in to the water column at a consistent frequency. Each instance of this pinging is referred to as an ensemble, and a typical frequency of sampling for these ensembles is 1Hz. The acoustic pings allow the ADCP to calculate the mean flow, or water, velocity (V_w) within measurement cells at multiple depths along a vertical using the same back-scattering Doppler shift principle as was mention previously in regard to the ADV. The ADCP transducer, which emits the sonic pings, will typically contain at least three separate beams that each emit a sonic pulse and allow for the the decomposition of the three-dimensional orthogonal velocity tensor, V_w, for the flow. The velocity of the moving boat, V_b, is also determined by the interaction of the sound waves with the bottom surface of the channel (or alternatively using GPS), and as such the distance between vertical ensembles is determined. The depth of each measurement cell within the vertical ensemble is determined by the user *a priori*.

The cell depth values are multiplied by the distance between vertical ensembles and the mean cell velocity to calculate a differential discharge value for the cell. The measureable discharge is then determined by integration of differential cell discharge values across the entirety of the channel cross-section. However, due to the nature of interacting sound waves from multiple transducer beams near the boundaries of the channel, extrapolation of the discharge is necessary in these areas near the channel boundaries. The particular method for extrapolation is left to be determined by the user, however manufacturer defaults typically assume a constant velocity profile near the water surface, and a logarithmic profile near the channel bed.

The ADCP represents a relatively time-efficient and accurate method for quantifying mean steady discharge in open-channels, so long as a large majority of the flow is directly measurable and not subject to extrapolation. Furthermore, ensuring that the measurement duration is sufficient to resolve an accurate estimation of the mean value of the fluctuating turbulent velocity field is critical for the correct usage of the instrument [11].

2.2.3 Hydraulic Structures and stage-discharge relationships

Velocity-area methods utilizing point velocity current meters or the ADCP represent viable options for quantifying streamflow in an open-channel if performed diligently and with adherence to relevant best practice guidelines. However, it is not practical to perform these methods each time a discharge measurement is desired. If frequent observation of flow quantity is necessary at a certain cross-section within a channel the most reasonable solution is the construction of a permanent hydraulic structure within the channel. These devices are typically placed within a prismatic rectangular channel so that estimations of discharge can be accomplished using theoretical relationships between stage and discharge. The presence of this structure represents an obstructive element within the flow that causes the deceleration of the fluid, and as such a loss in kinetic energy and associated gain in potential energy. This results in an increase in the depth of the flow upstream of the structure. Typically, these structures are situated in channels of mild bed slope, and thus the flow upstream of the structure assumes a "M2" or "backwater" water surface profile.

Backwater profiles represent deep, slow-moving flow with little fluctuation in the water surface due to the flow regime being sub-critical. This type of flow profile facilitates the accurate gauging of the flow depth, or stage, upstream of the structure. Possible options for stage measurement include stilling wells or pressure transducers. Although the primary focus of this work is the determination of discharge within irrigation canals, the measurement of stage also represents a critical aspect of overall flow quantification. Please see chapter six in Herschy (2009) for a discussion of relevant stage measurement methods for open-channel flow. [10].

The determination of stage upstream of a hydraulic structure is used for input to a stage-discharge rating equation that is specific to each type of structure. For the context of measuring flow within irrigation canals, the most common types of hydraulic structures used are weirs and flumes [10]. These devices are designed to force the flow through a certain state by which the theoretical determination of the discharge becomes a simpler task. Certain structures, such as broad-crested weirs or Parshall flumes, utilize the concept of critical depth. The flow transitions from sub-critical to super-critical as it passes through the structure, and as such a critical depth control is created [12]. Being able to assume a state of minimum specific energy allows simplifying assumptions to be evoked and discharge to be computed. Other structures, such as the sharp-crested weir, model the flow as an orifice discharging into a free overfall, whereby simplifying assumptions related to Torricelli's principle can be utilized. [13].

The derivation of theoretical rating equations for use in developing a stage-discharge relationship involve several simplifying assumptions, such as inviscid flow or a perfectly hydrostatic pressure distribution. In practical applications, these fundamental assumptions are severely violated and as such, semi-empirical correction factors are introduced. The specific values for these corrective factors, or discharge coefficients, have been established for well-studied structures such as the sharp-crested weir. In these cases, a user may well assume a commonly held value for the discharge coefficient and be able to gain an accurate estimation of flow rate. However, performing a unique calibration for a specific structure, even if it is of a popular type, is prudent to ensuring the highest possible accuracy in discharge estimation. Additionally, for certain novel structures that have not been the subject of as rigorous empirical study, calibration of the discharge coefficient is necessary through the use of a secondary flow measurement device. For this reason, the aforementioned velocity-area methods are frequently used as a means for calibrating hydraulic structures.

2.3 The stage-discharge rating equation for pivot weirs

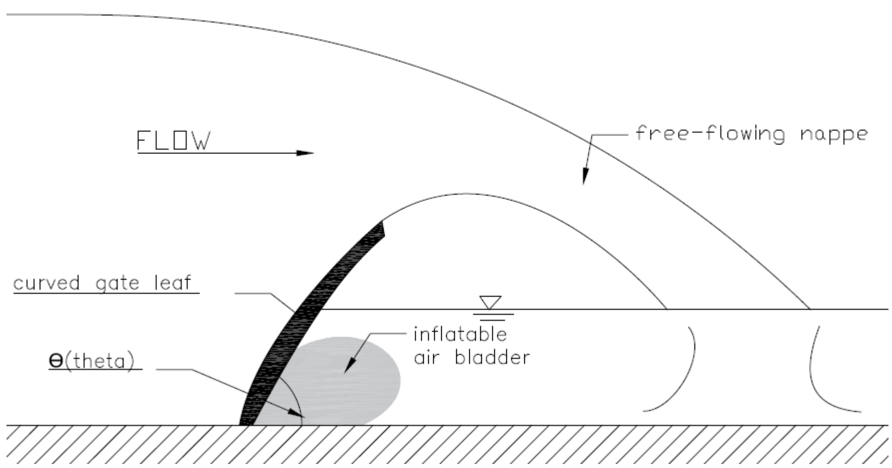

Figure 2.5: Generalized sketch of an Obermeyer pivot weir (structure components not drawn to scale).

One structure of particular interest for the context of irrigation water management is the Obermeyer pivot weir. This device was primarily designed as a means for managing upstream water depth levels to ensure sufficient available head for diversions into farm laterals. However, it can be considered a general purpose water level control apparatus. [14]. It consists of a curved gate leaf supported by inflatable rubber air bladders. the structure sits within a rectangular concrete channel and its bolted into a concrete foundation, as seen in Figure 2.5. The device is termed a pivot weir because the inclination angle of the gate can be adjusted by changing the inflation level of the air bladders. This is done using air compressors housed in an adjacent control unit, which is powered by solar panels to allow for remote field operation.

Although the primary purpose of Obermeyer pivot weir is as a stage management device, current attempts are being made to establish an empirical stage-discharge relationship for the structure

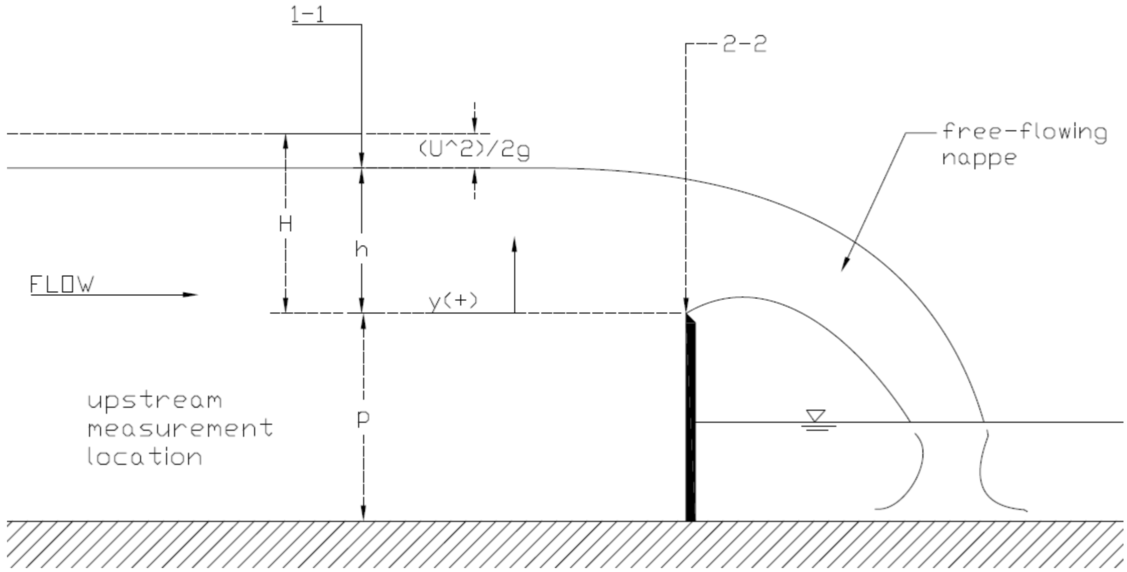

Figure 2.6: Schematic of flow over a sharp-crested weir.

for purposes of flow measurement. Currently, the relevant literature contains a modest amount of studies pertaining to the nature of the theoretical rating equation for a generalized pivot weir - which in essence is a flat thin plate set at an inclined angle adverse to the flow direction. Current attempts of rating the pivot weir have thus far have treated it as a special case of the sharp-crested weir. However, the validity of this approach deserves a healthy amount of skepticism, as the process of rating of the sharp-crested weir already involves a large amount of correction for violated assumptions. Here, the derivation of the original sharp-crested weir rating equation is explained for the purpose of highlighting the simplifying assumptions implicit in its derivation. Then, most relevant applications of this equation in attempts for application for a theoretical pivot weir rating equation are reviewed.

2.3.1 Foundation: The sharp-crested weir rating equation

The simplest and most widely used of all hydraulic structures is the fully-suppressed sharp-crested weir. It consists of a thin flat plat set perpendicular to the direction of the flow and spans the entire width of the channel. The crest of the weir is tapered so as to resemble a "knife's edge", so that the flow springs from the crest in a similar manner to flow through a sharp orifice.

Giovanni Poleni (1683-1761) is the individual first credited with deriving a rating equation for the sharp-crested weir after observing the orifice-like flow over the weir crest and relating the same phenomena to Torricelli's principle of fluid exiting a large static reservoir [8] In his observations, Poleni described two types of flow near the weir: "vivid" and "dead" water. He hypothesized the fluid below the crest of the weir, p - see Figure 2.6 could be treated as static or dead water. Only the depth of flow above the weir crest, h, he observed as vivid, or flowing dynamically [15]. As such, the sharp-crested weir acted like an orifice capped by the free surface. The depth of the flow upstream of the crest served as the supply reservoir of pressure head to drive the flow over the crest. Poleni's equation can be derived by applying Bernoull's principle along a series of streamlines between the upstream static location and the crest:

$$\frac{P_{1-1}}{\gamma} + \frac{{U_{1-1}}^2}{2g} + h_{1-1} = \frac{P_{2-2}}{\gamma} + \frac{{U_{2-2}}^2}{2g} + y_{2-2}; \tag{2.4}$$

or, more generally:

$$\frac{P}{\gamma} + y + \alpha\frac{\overline{U}^2}{2g} = H. \tag{2.5}$$

Here, H is the total mechanical energy head of the flow, which in Bernoulli's equation is assumed to be constant. $\frac{P}{\gamma}$ is the pressure head, where P is pressure in units of force/area $[ML^{-1}T^{-2}]$, and γ is the specific weight of the fluid $[ML^{-2}T^{-2}]$. y is the elevation head above a fixed datum, which in Eq. (2.4) is taken to be elevation of the crest. $\alpha\frac{\overline{U}^2}{2g}$ is the velocity head, where $\overline{U}$ $[LT^{-1}]$ is the average flow velocity in the channel, and g $[LT^{-2}]$ is the gravitational acceleration coefficient. α is the kinetic energy correction factor that accounts for non-uniform velocity distributions in the channel cross-section, defined as [16]:

$$\alpha = \frac{\int u^3 dA}{\overline{U}^3 A}. \tag{2.6}$$

The first assumption made in the sharp-crested weir rating equation derivation is that the pressure at both sections is assumed hydrostatic and thus neglected. It also follows that the pressure underneath the nappe as it flow overs the crest is atmospheric. The velocity head at the upstream section 1-1 is also neglected under the assumption of slow-moving sub-critical flow. Rearranging to solve for the velocity at an arbitrary point along the crest:

$$U_{2-2} = [2g(h_{1-1} - y_{2-2}]^{1/2}; \tag{2.7}$$

and multiplying the RHS of (2.7) by the channel width, b, and integrating along the depth of the crest from the datum of the crest height, p to the upstream head, h_{1-1} yields an estimation of volumetric flow rate. This approach assumes negligible draw-down from section 1-1 to section 2-2:

$$Q = \sqrt{2g}b \int_0^{h_{1-1}} (h_{1-1} - y_{2-2})^{0.5} dz. \tag{2.8}$$

Finally, integrating and replacing h_{1-1} simply with h_1, we have the well-known Poleni weir equation:

$$Q = \frac{2}{3}\sqrt{2g}bh_1^{3/2}. \tag{2.9}$$

In summary, the simplifying assumptions used for the derivation of Eq. (2.9) are:

- The pressure field in the flow is completely hydrostatic (streamlines perfectly horizontal).
- Pressure underneath the nappe is atmospheric.
- The fluid is inviscid and irrotational.
- The upstream kinetic energy head is negligible.
- There is no significant draw-down between upstream and crest water surface elevation.

Due to the fact that many of these assumptions are violated under practical applications, a corrective discharge coefficient, C_d, is introduced. This coefficient is non-dimensional and represents a ratio of the energy that is retained between the upstream and crest sections compared to the ideal inviscid case. As such, C_d will be < 1, typically taken as a value between 0.7-0.75 for

$0.6 \leq h_1/p \leq 2$ [17, 18]. Eq. (2.9) then becomes:

$$Q = \frac{2}{3} C_d \sqrt{2g} b h_1^{3/2}. \tag{2.10}$$

2.3.2 Adaptation: Wahlin and Replogle (1994)

The seminal study in determining a rating equation for the pivot weir was completed by Wahlin and Replogle (1994). In this study, tests were performed on two laboratory models of pivot weirs. The first weir had a crest width, b equal to 1.2m, with a gate length, L_g of 0.61m. The second structure had b = 1.14 m, and L_g = 0.46m. The authors began with the assumption that the general form of the sharp-crested weir rating equation, Eq. (2.10), could be applied to the rating of pivot weirs after an additional corrective factor to account for changes in gate angles was introduced (C_a). The form of the rating equation established by Wahlin and Replogle is:

$$Q = \frac{2}{3} C_a C_e \sqrt{2g} b_e h_e^{3/2}. \tag{2.11}$$

Here, the discharge coefficient accounting for the violated assumptions within the sharp-crested equation is given by a variation on the Rehbock equation published in [16]:

$$C_e = 0.602 + \frac{h_1}{p} 0.075. \tag{2.12}$$

Therefore, Eq. (2.11) assumes that the discharge capacity of the structure is a function of the elevation head of the water above the weir crest, p, and will increase as the depth increases. Similarly, Eq. (2.11) incorporates "effective" parameters for the width and upstream head values, in accordance with the guidance of Kindsvater and Carter (1959) [19] to account for viscous and surface tension effects at low heads. For a fully-suppressed sharp-crested rectangular weir these values are:

$$b_e = b - 0.001\ m; \tag{2.13}$$

$$h_e = h_1 + 0.001\ m. \tag{2.14}$$

By observing data previously collected by the US Bureau of reclamation (USBR) for the study of crests for overfall dams, the authors hypothesized that the relation between C_a and the gate inclination angle, θ, would take the form of a second order concave polynomial. The coefficient C_a can also be thought of as a discharge amplification factor, Q/Q_{90}, that represents the effect of the gate angle, θ on amount of discharge that is able to pass through the structure at a given head. The results of the study proved to be fairly true to the original hypothesis, and a second order polynomial for C_a was defined as:

$$C_a = 1.0333 + 0.0038848\theta - 0.000045\theta^2; \tag{2.15}$$

where θ is the gate angle in degrees. In conjunction with Eqns. (2.11) and (2.12), the authors claimed that developing a stage-discharge rating curve for pivot weirs using Eq. (2.15) was accurate to 6.4% when applied to field-scale pivot weirs, for $h/p < 1$ and $16.2° \leq \theta \leq 63.4°$ [20]. However, the empirical nature of the C_a deserves further exploration. Additionally, the author's use of the modified Rehbock equation (2.12) for determination of C_e may be another source of error. More recent studies have shown that the discharge coefficient within the operational range of the sharp-crested weir should not vary significantly with h/p [17, 18, 21].

2.3.3 Novel approaches: Bijankhan, Ferro, and Di Stefano (2018)

In an attempt to develop a generalized theoretical approach for stage-discharge relationships of rectangular weirs with different contraction ratios, Bijankhan, Di Stefano and Ferro (2018) utilized dimensional analysis and incomplete self-similarity theory to develop a non-dimensional rating equation of the form [18]:

$$\frac{k_s}{p} = a(\frac{h}{p})^m. \tag{2.16}$$

Here, m for a rectangular weir can be assumed as unity, where a is dependent on the geometric properties of the weir. It is unitless and can be considered a transformed discharge coefficient.

Then, Eq. (2.16) simply represents a rearranged presentation of (2.10), where:

$$k_s = \frac{Q^{2/3}}{b^{2/3} g^{1/3}}; \tag{2.17}$$

is the critical depth [L], and a in (2.16) is related to C_d by:

$$C_d = \sqrt{\frac{9a^3}{8}}. \tag{2.18}$$

Due to the non-dimensional nature of this approach, a constant discharge coefficient is assumed that is independent of h/p. This eliminates the need for incorporating an effective discharge coefficient, such as is the approach in the Rehbock equation (2.12). The calibration of the coefficient a can be used to reflect the changes of gate inclination angle on the classical sharp-crested weir rating equation. Towards this purpose, the authors investigated a laboratory model pivot weir of b=0.6 m with $0.232m \leq p \leq 0.309m$ at four different gate angles with $4.65L/s \leq Q \leq 46.4L/s$. They discovered a similar trend compared to Wahlin and Replogle (1994) in regard to the relationship between the gate angle, θ, and the flow amplification factor, Q/Q_{90} with an average agreement of 6.7% [22]. However, the nature of the mathematical relationship between C_a and θ remains ambiguous. Wahlin and Replogle (1994) predicted it to be a second order concave polynomial (2.15). Bijankhan and Ferro (2018) estimate the trend as a rational function of the following form:

$$a = \frac{206.9 + 0.801\theta^{-21.348}}{272.25 + \theta^{-21.348}}; \tag{2.19}$$

where a is the rearranged discharge coefficient found in (2.16). Hence, there is currently disagreement in the current literature on the nature of the mathematical relationship between the angle of inclination of the pivot weir and the discharge coefficient, specifically - whether this relationship is monotonic. Further investigation is then required, along with a more descriptive explanation of the range of h/p and θ values for which using the pivot weir as a flow measurement device is viable.

2.4 Summary

This chapter has introduced the basic governing equations related to flow quantification in open-channels, along with a brief description of the major types of measurement commonly used in irrigation canals. Furthermore, the nature of the stage-discharge rating equation for pivot weirs was explained. The next chapter describes original research done for the purpose of investigating methods for reducing uncertainty in ADCP discharge methods.

Chapter 3

Refining protocols to mitigate user-induced uncertainty in ADCP moving-boat discharge measurements in irrigation canals

3.1 Study Overview

[2]A *Teledyne RD Instruments StreamPro* ADCP was used to quantify flow rates in manmade irrigation canals with the aim of determining best practices for: the method of deployment of an ADCP using a moving boat, the duration of the measurement transect per unit width of canal, and the number of transects to use in computing mean steady discharge. The purpose of these refinements is to lessen user-induced uncertainty and to estimate the point of diminishing returns for additional data collection. Suggested protocols developed from this experimentation indicate that a reduction of 30 to 70% in the values of uncertainty metrics can be accomplished utilizing a remotely operated tagline deployment method with a minimum transect duration relative to the canal top width of 24 s/m (7.3 s/ft), equivalent to 24 vertical pings per meter of an ADCP measuring at 1 Hz. Furthermore, at least six total transects taken in reciprocal directions are recommended for measurements of mean steady discharge. The conclusions of this experimentation will equip ADCP users within all ranges of experience with further guidance to achieve more reliable flow quantification and hydraulic structure calibration.

3.2 Introduction

It has become standard practice when conducting hydraulic flow experiments to quantify an interval of uncertainty within which the true value of a measurement is believed to reside. This al-

[2]The results presented in this chapter have been submitted in substantial part for publication in the journal *Flow Measurement and Instrumentation* with co-authors Timothy K. Gates and S. Karan Venayagamoorthy.

lows experimentalists to operate with a quantifiable metric of data quality, i.e. the relative width of the uncertainty interval associated with the measurement. Beyond this, incorporating uncertainty analysis into experimental hydraulics provides an opportunity to innovate new ways to lower this uncertainty, and facilitates integration of streamflow data from multiple providers [23]. Uncertainty mitigation can be conducted in all phases of an experiment (i.e. design, execution, and post-processing) [24]. The purpose is to provide scientists and engineers with a notion of the degree of confidence in their measurements and to enhance accuracy in measuring flow phenomena that are crucial to the efficient management of a system. Better knowledge of how to improve data quality drives innovation [25], and also has been identified as a key principle to incorporate into institutional frameworks aimed at pursuing sustainable development [26] because it helps reduce costs and promotes robust decision making [5]. In the context of measuring flows for irrigation water management, it is essential that ambiguity in measurement is diminished in systems strained by water scarcity brought about by increasingly frequent drought and by rapid growth in population and demand for food supply [27].

These motivations have made the reduction of uncertainty associated with measuring streamflow using an Acoustic Doppler Current Profiler (ADCP) an area of particular interest. The ADCP is a flow measurement device that utilizes the Doppler effect by emitting ultrasonic pulses sent into a body of moving water containing particulate matter that reflects the pulses [11]. This method is far more time-efficient than the typical section-by section velocity-area method of streamflow quantification [28]; thus, the ADCP allows measurement on temporal and spatial scales that previously have been unachievable. The relative ease of use of the ADCP has made it a favorite choice among hydrographers such that, as of 2013, 98% of all United States Geological Survey (USGS) streamflow measurements in non-wadable streams were made using an ADCP [29]. Additionally, ADCP flow measurements frequently are used internationally for research in irrigation and agricultural water management [30–32].

3.2.1 Identification of sources of uncertainty associated with ADCP measurement and mitigation strategies

A fundamental issue in employing any device, in this case an ADCP, to gauge flow rate is that the measurement is subject to uncertainty that arises from several sources. Moreover, a secondary benchmark measurement of the "true" (or "truer") discharge is rarely available for comparison, especially in a field setting. Instead, users are faced with the challenge of doing their utmost to reduce the overall uncertainty in their measured discharge in hopes that shrinking this band of uncertainty will bring them a closer estimation of the true discharge.

Although an ADCP offers time efficiency, enhanced precision, and ease-of-use improvement over traditional flow measurement methods, it is far from being a perfect instrument. The types of uncertainties associated with ADCP measurement have been compiled and thoroughly discussed [33]. For example, the ADCP suffers from an inability to directly measure the entirety of the cross-sectional area of the flow; thus, the instrument must extrapolate on the nature of the flow outside its gauging capacity. The danger of this approach is that it assumes the nature of a phenomenon that is beyond the limits of observation, a basic scientific pitfall [34]. Furthermore, it has been shown that the entrance of the ADCP transducer into the flow results in a disruptive effect, tending to bias low the velocity readings near the water surface [35, 36]. To summarize, the elemental sources of uncertainty can be grouped as: instrument characteristics and operational settings, analytical methods for estimating physical quantities, measurement approaches and protocols, the physical conditions of the measurement environment (including inherent spatiotemporal variability), and operator skill [37]. Altogether, this constitutes a form of Type B uncertainty in the measured value, as described in [38]. Type B uncertainty is dealt with by assigning probability distributions and selected statistics, that are estimated from available data and scientific judgment, to describe probable errors that lie within an inter-percentile band around a measured variable [39, 40]. A variable's true value is taken to be equal to the measured value at any space-time location plus an error, which could be either positive or negative. The true value has been described as lying within "a probable error range" [41]. Though this band of uncertainty cannot be eliminated, steps can be taken to reduce it. The challenge is to discover the point of diminishing returns in reducing uncertainty from one or more sources.

The current peer-reviewed literature on mitigation strategies for identifying and reducing uncertainty in hydro-acoustic measurements is rich. Recent efforts have focused on a variety of approaches, including: standardizing computational algorithms for data filtering and quality assessment [42], developing theoretical and semi-empirical models of uncertainty from a standardized statistical basis [33, 37, 43], and performing carefully designed field and laboratory experiments aimed at quantifying the uncertainty of an ADCP measurement with respect to a trusted reference [44–48].

3.2.2 Study aim and approach

The goal of this present study is to provide further insight towards strategies for the mitigation of uncertainty in moving-boat ADCP discharge measurements derived from "measurement approaches and protocols". We apply statistical measures of uncertainty to experiments with ADCP measurements in the field to point toward recommended protocols for deployment method for a moving-boat, the relative duration of a single transect, and the number of transects to employ (see Figure 3.1).

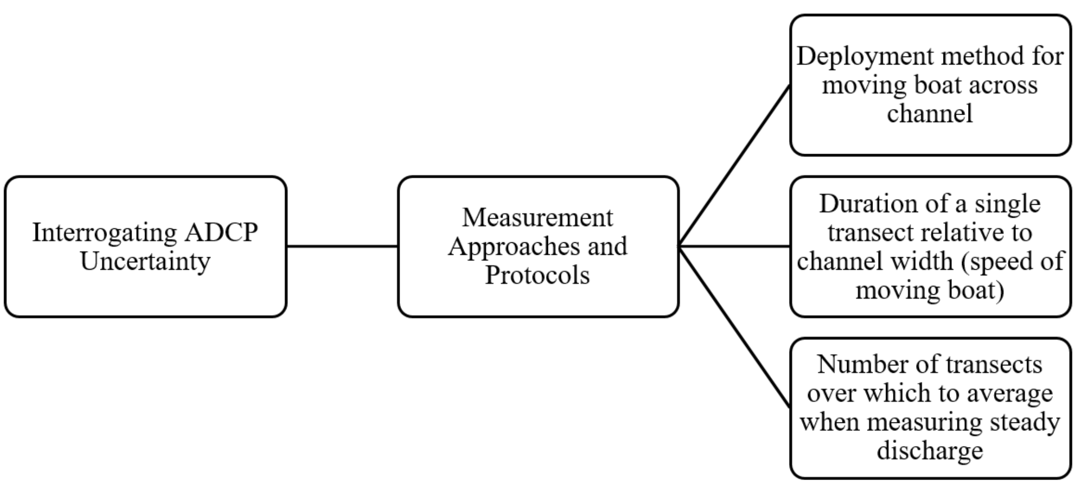

Figure 3.1: Diagram of study aim

Additionally, complementary discussion on the current literature is provided concerning aspects of site selection. Although ADCP operational best-practices for sampling time and number of reciprocal transects vary somewhat internationally [46], the most widely-followed guidelines were established by the USGS in 2007 by the seminal work of Oberg and Mueller [11, 49]. This guidance document was last updated in 2013 and includes extensive information on best practices for measuring discharge using an ADCP. These guidelines correspond to a recommended minimum total sampling time of 720 seconds (with no reference to the size of the stream), and the collection of at least two transects taken in reciprocal directions in order to avoid any directional bias in the flow. The guidelines also note that the sampling time of the measurement is likely a more significant factor than the number of transects included. The speed the boat moves across the transect is recommended to be "relatively uniform", at less than or equal to the average water speed, and slow enough to collect a sufficiently large amount of data without sacrificing the smoothness of boat operation. These "rule-of-thumb" guidance statements can at times seem contradictory. In this study, we identify the issue with these best-practice guidelines being the ambiguity as to the proper speed of the moving boat under a variety of channel widths, which has been identified as an important parameter contributing to uncertainty [33]. This lack of clarity in the guidelines runs the risk of resulting in unnecessarily long measurement time in smaller channels, and more importantly, the risk of far too short a time in larger canals and streams. Furthermore, insufficient duration in measurement could lead to a decrease in data quality for especially turbulent flows where the timescale of the largest eddies is longer than the time spent observing the flow with the ADCP. An attempt is made herein to prescribe a recommended range for individual transect sampling duration relative to the width of the channel, as well as to clarify the recommended number of transects to average across when determining mean discharge of steady flow in irrigation canals.

3.3 Instruments and Methods

3.3.1 Study Location

Field experiments were carried out during the summer of 2020 within the Larimer and Weld Irrigation District east of the Cache la Poudre River near Fort Collins, Colorado, USA (Figure 3.2). A total of four measurement locations were selected based upon criteria of accessibility, canal width, favorability for ADCP measurement, and flow rate. The aim was to find a balance between choosing earthen irrigation canals that varied by width, environmental conditions affecting measurement uncertainty (i.e., vegetation, bed material, susceptibility to wind effects, etc.), and flow rate; with the accompanying goal of obtaining a large enough dataset such that comparison among observations taken at the same location would be viable.

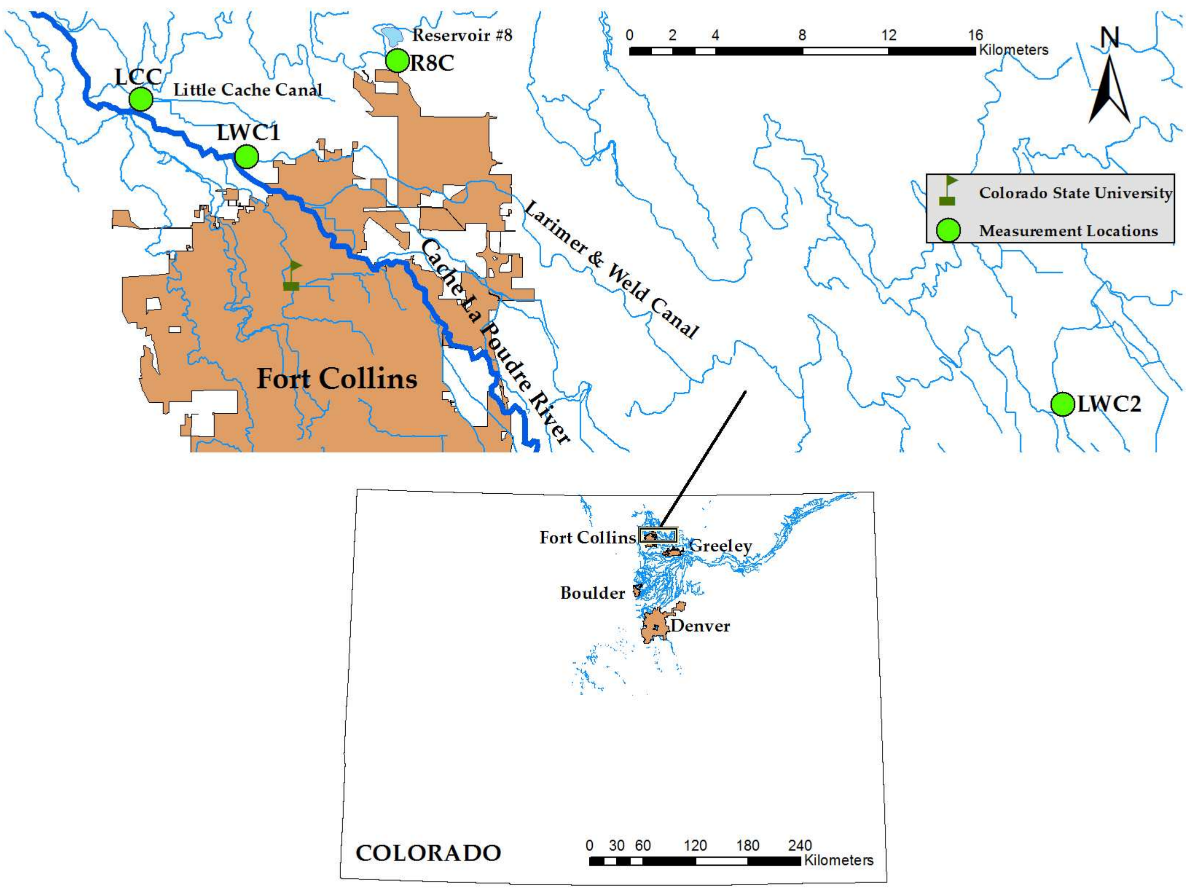

Figure 3.2: Diagram of study area

Table 3.1 lists the characteristics of the canal locations where ADCP measurements were made, and Figure 3.3 provides site photos of the measurement locations.

Table 3.1: Characteristics of measurement locations. The number in parentheses for LWC2 signifies transects taken using a manual rope-and-pulley deployment method.

Measurement Location	Abbreviation	Avg. Q (m^3/s),(cfs)	Avg. % flow rate directly measured (Q_m/Q_{total})	Avg. width (m)	Avg. Cross-sectional area (m^2)	Total No. single transects analyzed	Avg. Cell depth (cm)
Reservoir #8 Outlet	R8C	0.53 (19)	63.9	6.27	3.87	70	4
Little Cache Canal	LCC	1.81 (64)	54.9	5.59	2.19	108	2
Larimer & Weld Canal Site 1	LWC1	6.97 (246)	60.3	14.70	8.51	28	4
Larimer & Weld Canal Site 2	LWC2	6.24 (220)	76.2	11.89	13.33	108 (136)	7

3.3.2 ADCP settings and quality assurance

The type of ADCP used for experimentation was a *StreamPro* manufactured by Teledyne RD Instruments with an output frequency of 1 Hz for the average velocity in each measurement cell within the channel cross section. Two ADCP probes were used in this study (Serial No. 861 at LCC and LWC1; Serial No. 567 at R8C and LWC2), both of which were verified to be in good agreement with streamwise velocity readings of a Laser Doppler Anemometer in a laboratory flume during a 2018 study [47]. Best practices for routine maintenance, transport, and storage of the ADCPs were followed per guidance established by USGS [50]. Water mode 12 was used for all measurements, as no slow-moving or very shallow flows were observed. A moving bed test was completed at the beginning of each day of measurement, or when large changes in the canal flow regime were observed. No notable moving bed effects were detected. Additionally, an automated

Figure 3.3: Photo of measurement locations. Clockwise beginning at top left: R8C, LCC, LWC1, and LWC2. View is upstream.

ADCP systems check was performed before measuring discharge to confirm that the instrument was functioning normally. Beam #3 of the ADCP was oriented 45 degrees and forward towards the upstream direction, following guidelines established by Teledyne RD Instruments [51]. The depth of the ADCP measurement cell was chosen by taking an a priori measurement of maximum canal depth by wading using a staff gauge. This maximum depth was then divided by the maximum number of cells per ADCP ensemble (either 20 or 30 depending on ADCP used) to estimate the cell depth size that would provide the highest possible measurement resolution under the given conditions. Finally, an independent measurement of water temperature was taken using an In-Situ *SmarTroll* multi-probe at the beginning of the day of measurement to ensure that the *StreamPro* temperature sensor was within at least 2 °C of the independent temperature reading, per recommendations established by USGS [42]. This is done so the ADCP calculations of velocity, which are dependent on the properties of sound propagating through water, can be validated.

3.3.3 Data Collection and Management

Data were collected with the ADCP and subsequently processed using the manufacturer's *WinRiver II* software, version 2.20. Field notes were taken to record measurement location characteristics such as vegetation; weather; flow regime, and qualitative observations of turbulent structures. Before recording experimental data, a trial transect was measured to limit any start-up errors that may have influenced the measurement. A pre-selected number of transects, ranging from four to twelve depending on the measurement location, were collected under a pre-determined set of parameters for boat speed and the boat deployment method. Hereinafter, this collection of an even number of transects with specific procedural parameters, over which a mean discharge value is determined, is referred to as a single "experiment". A transect measurement was designated as an outlier if some erroneous condition occurred during measurement, such as a malfunction in the ADCP motion across the tagline, loss of battery power to the ADCP, or submergence of the ADCP due to excessive surface waves. However, these occurrences were very rare. Additionally, the velocity contour plots were qualitatively examined in *WinRiver II* to ensure that no excessive bottom tracking errors were present and that edge discharges were estimated accurately. Flow was determined to be nominally steady with measurements of stage recorded at a frequency of every 5 minutes. During the duration of discharge measurement, variations in stage did not exceed +/- 6 mm (0.02 ft), in all cases equivalent to $\leq 0.7\%$ of the flow depth. Experiments were designed to investigate the parameter of relative transect duration. A typical day at a site included triplicate measurements of flow rate at the same location, performed at "slow", "intermediate", and "fast" speeds of boat travel. Two different systems of deployment were explored for moving the boat across the transect. At locations LWC1, LCC, and R8C, a remotely operated tagline deployment system - the *ADCP Traveler*, manufactured by NIWA Instrument Systems, was solely used. At LWC2, both the *ADCP Traveler*, and a manually-operated rope-and-pulley system were used and carefully compared. The *ADCP Traveler* is marketed as an improvement upon manual deployment methods because it offers smoother operation of the boat at a more constant boat speed. Figure 3.4 is included to illustrate the marked difference in an ability to maintain a steady boat speed between the two deployment methods.

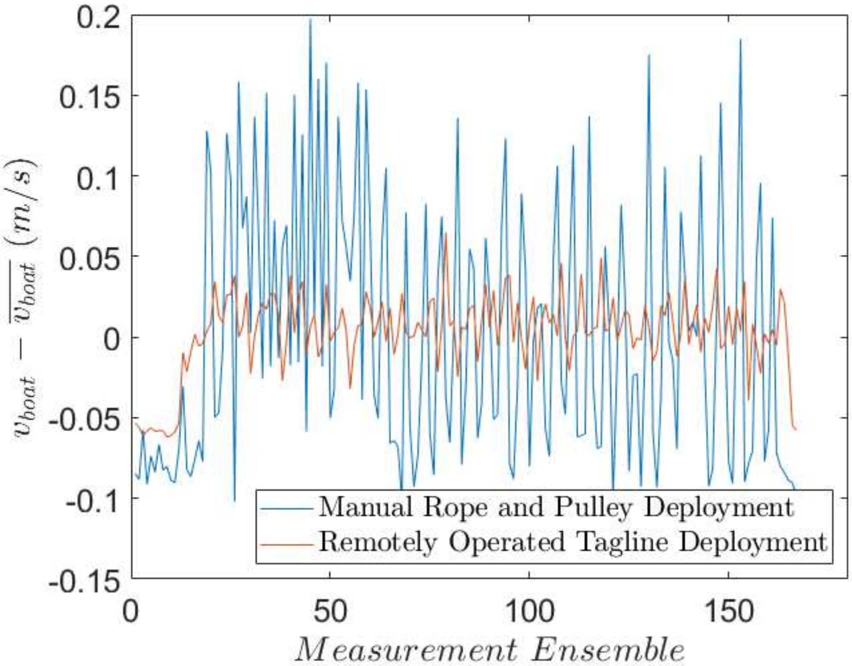

Figure 3.4: Comparative plot showing the instantaneous signal of ADCP moving boat speed, $v_{boat}(m/s)$, relative to its average for the transect, $\overline{v_{boat}}(m/s)$, for two distinct transects measured at the same approximate relative duration using different deployment methods.

All data filtering, smoothing and extrapolation for unmeasured regions of the canal cross-section were done using the default algorithms present within WinRiver II. Post-processing was also completed within the software, where then ASCII files with necessary data were generated for external analysis in MATLAB (r2020a). At two measurement locations, LWC1 and LCC, a nearby (within 20 m) independent discharge measurement using a rated structure was available per the Colorado Division of Water Resources (CDWR). The average percent difference for the ADCP readings from the rated discharge reported by the CDWR at LWC1 and LCC were only 3.6% and 8.3%, respectively.

3.3.4 Deployment method and relative duration parameters

To investigate the boat deployment method and the relative duration of a transect (RD_t), ADCP discharge measurements were analyzed for uncertainty following the procedure described by H. Huang of Teledyne RD Instruments [52]. RD_t is calculated by dividing the time it takes the ADCP to traverse from bank to bank across the canal by the top width of the canal. The method of Huang was chosen because it constitutes a measure of uncertainty for straightforward application to field ADCP streamflow measurements made using a moving boat. In this approach, the relative standard uncertainty in the measurement of discharge over a single transect is calculated as:

$$RSU_m = s_Q / c\overline{Q_m}; \tag{3.1}$$

where s_Q is the sample standard deviation in the number of transect measurements of Q_m, which is the directly-measured discharge (excluding extrapolated discharge within portions of the canal cross section not directly measured by the ADCP) per experiment; $\overline{Q_m}$ is the mean of Q_m over the experiment; and c is the bias correction factor for s_Q . This approach addresses uncertainty associated with measurement protocol and is not confounded by other large sources of uncertainty, such as near-bed/transducer extrapolation or edge discharge errors. The value of c in (3.1) is calculated as

$$c = \frac{\sqrt{\frac{2}{n_{t_e}} - 1} \cdot \Gamma(\frac{n_{t_e}}{2})}{\Gamma(\frac{n_{t_e}-1}{2})}; \tag{3.2}$$

where Γ is the Gamma function, and n_{t_e} is the number of transects per experiment. The ratio s_Q/c can be considered as the mean-unbiased estimator of the population standard deviation. Thus, RSU_m is equivalent to the coefficient of variation of the directly-measured discharge [52], and provides a measure of relative uncertainty for comparisons between alternative boat deployment method and RD_t protocols.

Since only a single value of RSU_m was calculated per experiment, the sample size of RSU_m was small for most measurement locations and could not be confirmed to approximate a normal distribution. Therefore, to test for the statistical significance in outcomes between alternative methodological protocols, a measure of uncertainty following a roughly normal distribution and with a sufficiently large sample size was needed. The relative residual error of a single transect measurement of discharge was chosen, defined as:

$$RRE_{m,i} = \frac{Q_{m,i} - \overline{Q_m}}{\overline{Q_m}}; \tag{3.3}$$

where $Q_{m,i}$ is the measured discharge for an individual transect, and as before, $\overline{Q_m}$ is the mean of the measured discharge over all individual transects within an experiment. An experiment is a collection of an even number of individual transects (i.e. paired at four, six, eight, ten, or twelve transects). To determine if a particular change in operational protocols resulted in a significant change in uncertainty, we use the variance in the distribution of RRE_m as proxy for uncertainty. It is expected that protocols associated with greater uncertainty will have a wider variance by which the residual errors of individual transect measurements are distributed. Variance in RRE_m is:

$$var(RRE_m) = \frac{\sum(RRE_{m,i} - \overline{RRE_m})^2}{n_{t_g} - 1}; \tag{3.4}$$

where $\overline{RRE_m}$ is the mean relative residual error of all transects within a group, and n_{t_g} is the number of transects within that group. A group can be defined as collection of experiments all falling under the same protocol constraints (i.e. measurements taken using a particular ADCP deployment method or prescribed RD_t). This uncertainty metric allows for the computation of a two-sample F-test, which determines if the variances between two independent and normally-distributed samples (in this case, two alternative groups of protocol choices) are significantly different. This test is one-tailed, under the assumption that groups with a longer RD_t, or completed using a remotely operated tagline deployment method, will have lower uncertainty. Additionally, a Kolmogorov-Smirnov test was completed to interrogate the normality of RRE_m distributions for each group. All distributions were found to be at least approximately normal. This complies with the statistical requirement that residual error in measurement, regardless of its variance, should be normally distributed around an approximate mean of zero. Hence, by first using the standard metric RSU_m to detect an impact of a particular protocol on relative measurement uncertainty, we were then able to test if this impact was significant between two groups by evaluating the more robust metric RRE_m.

3.3.5 Determination of recommended guideline for relative duration

To determine the minimum RD_t value needed to significantly reduce uncertainty in ADCP measurements, an initial estimate was made by analyzing visual plots of RSU_m with respect to RD_t. A minimum value was chosen by comparing the plots for the four measurement locations and identifying a cutoff below which uncertainty increases substantially. Then, this minimum value was tested for legitimacy in an iterative fashion by making incremental changes to the value until convergence was achieved by confirming that differences in the variance of RRE_m among the two groups containing data below and above the minimum RD_t value were statistically significant.

3.3.6 Number of transects per measurement of steady discharge

To analyze the uncertainty associated with an operator's choice of the number of transects (N_t) to employ when deploying the ADCP, we assume that the flow rate being measured is steady and that the accuracy of the experiment in relation to the true mean discharge increases with the number of observations. This assumption is fundamental to the nature of sample variance (Eq. (3.4)). If the flow is steady, including additional transects in the calculation of mean discharge should result in a reduction in uncertainty as the sample mean approaches the population mean. For the purposes of this study, we attempt to identify the point of diminishing return where including additional transects in computing the sample mean discharge does not result in a significant decrease in uncertainty. We define a measure of sample error that represents the percentage range on either side (+/-) of the sample mean within which the true population mean is expected to reside. It quantifies the relative difference between the sample mean and population mean and is defined as [53]:

$$E_s(\%) = \frac{|\overline{Q_m} - \mu_{Q_m}|}{\overline{Q_m}}; \tag{3.5}$$

where $\overline{Q_m}$ is taken to be the sample mean for a subset of transect discharge measurements within an experiment, and μ_{Q_m} is the estimated population mean for a large number of transect discharge measurements. Here, we estimate the population mean for an experiment as the mean discharge calculated using the maximum number of transects recorded, assuming that the sample mean approaches the population mean as the number of transect discharge measurements increases. Then, we define sample means for subsets of that experiment which contain a lesser number of transects for calculating $\overline{Q_m}$. We define N_t as the number of transects included in a computation of $\overline{Q_m}$. For example, the maximum number of transects collected per experiment at LWC2 was eight. We then determine E_s values for experiment subsets for which N_s equals two, four, and six transects, respectively. For purposes of simplification these subsets are delineated in the order in which the transect measurements were conducted. The metric E_s is determined for a grouping of experiment subsets that share the same value of N_t. The number of experimental subsets included in the calculation of median E_s is n_{s_g}. To determine if increasing the number of transects in an experiment significantly reduces E_s, we analyze distributions of E_s that are grouped by N_t and compare differences in the median value of E_s using a one-tailed two-sample Wilcoxon rank sum test. We use this nonparametric test due to the distributions of E_s containing only positive values and hence being heavily right-skewed [54]. The test is one-tailed under the assumption that as N_t increases, the median value for E_s will decrease.

3.4 Results

3.4.1 ADCP boat deployment method

The plots in Figure 3.5 illustrate the difference in the RSU_m values associated with two methods of deploying the boat containing the ADCP for traverse across the width of the canal at location LWC2. Irrespective of RD_t, measurements taken with the remotely operated ADCP Traveler tagline deployment method had an average RSU_m of 1.65% and a var(RRE_m) of 2.43e-04, whereas those taken using the manual rope-and-pulley deployment method had an average RSU_m of 2.87%, with a var(RRE_m) of 7.05e-04. Using a two-sample F-test, the difference in the variance

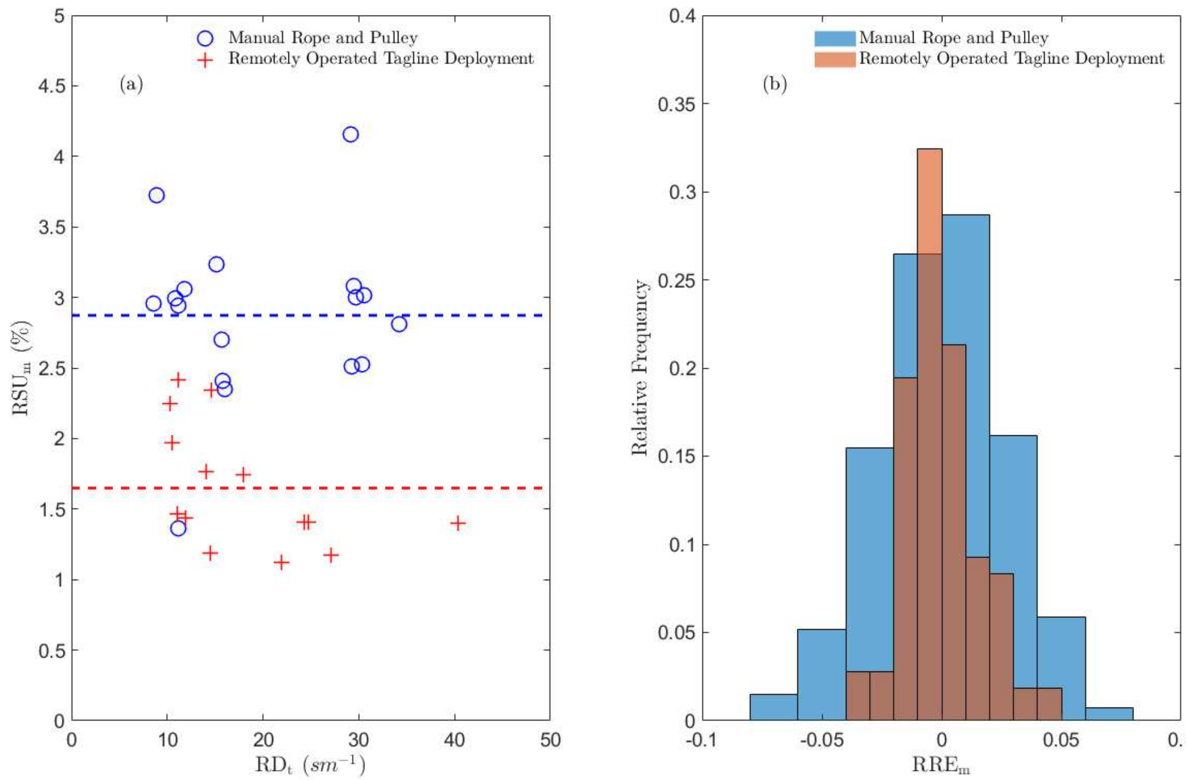

Figure 3.5: Plots of (a) RSU_m as a function of the RD_t for ADCP flow measurements at LWC2 using the remotely operated ADCP Traveler and a manual rope-and pulley-system (horizontal lines indicated the average RSU_m for each group.), and (b) corresponding relative frequency histograms of values of RRE_m .

between the two groups was statistically significant at a 5% level (p = 1.25e-08). It also can be seen from Fig. 4 that increasing RD_t when using the manual deployment system did not result in a reduction in RSU_m, as was the case with the remotely operated tagline method.

Using a remotely operated tagline deployment method with greater control over boat speed and steadiness resulted in an average reduction in the RSU_m uncertainty measure of 1.22 percentage points when compared to measurements taken using the manual rope-and-pulley method that is prone to unsteadiness in boat movement.

3.4.2 Transect relative duration

Figure 3.6 shows calculated RSU_m for experiments conducted at each location as a function of RD_t. The results are grouped by measurement location to avoid the confounding effects of site-specific sources of uncertainty on the data. The total number of individual transects per experiment used to compute the RSU_m values plotted in Figure 3.6 ranged from four to twelve, and the total sampling (exposure) times ranged from 726 s to 3900 s.

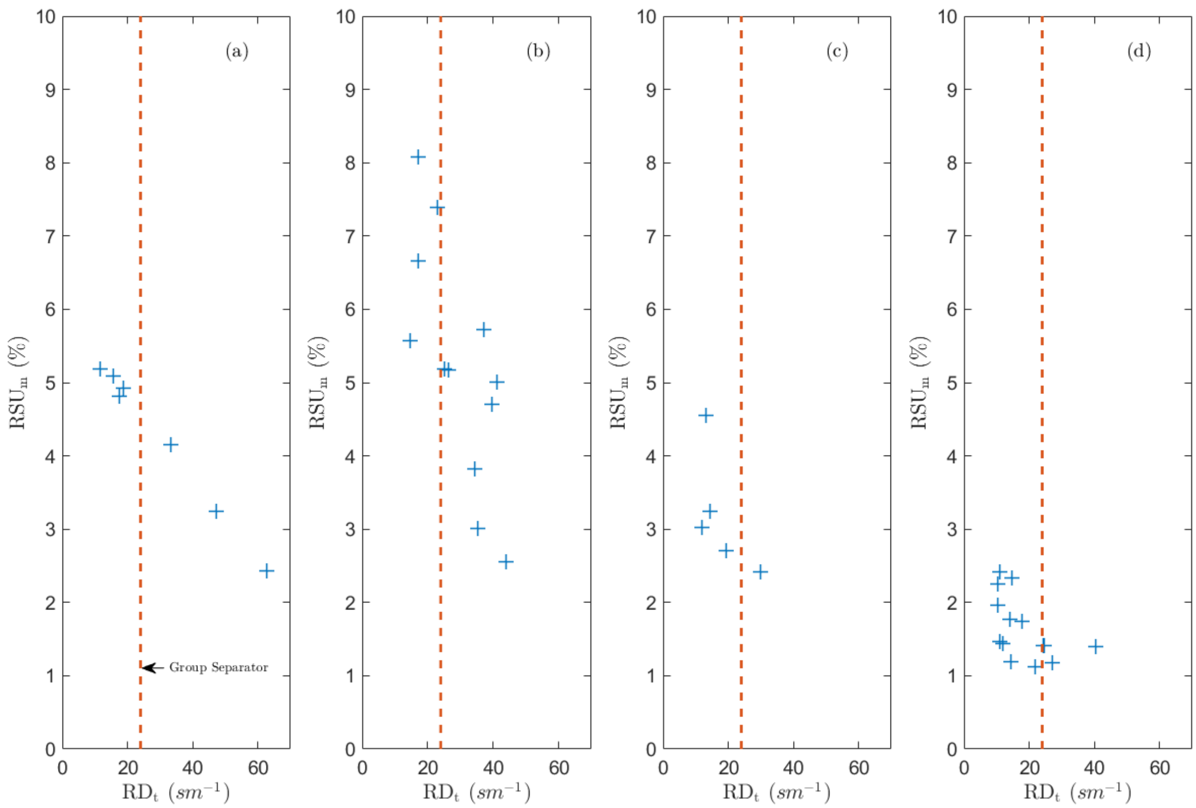

Figure 3.6: RSU_m plotted as a function of RD_t for locations: (a) R8C, (b) LCC, (c) LWC1, and (d) LWC2. The vertical group separator lines indicate the separation in data points below and above the recommended minimum RD_t of 24 s/meter.

A vertical line is included in each plot to illustrate the demarcation in RD_t grouping for each measurement location, representing a recommended minimum RD_t of 24 s/m width (7.3 s/ft), prescribed for a single transect in order to significantly reduce uncertainty in operational parameters. RD_t Group 1 represents transect data collected using an RD_t value less than the specified minimum of 24 s/m (7.3 s/ft), and in contrast, RD_t Group 2 contains transect data with an RD_t greater than the recommended minimum. A two-sample one-tailed F-test was run to determine if the observed difference in var(RRE_m) between the two groups was significant. The alternative hypothesis was that the variance in RD_t Group 2 would be less than that of RD_t Group 1. Results are summarized in Figure 3.7 and Table 3.2.

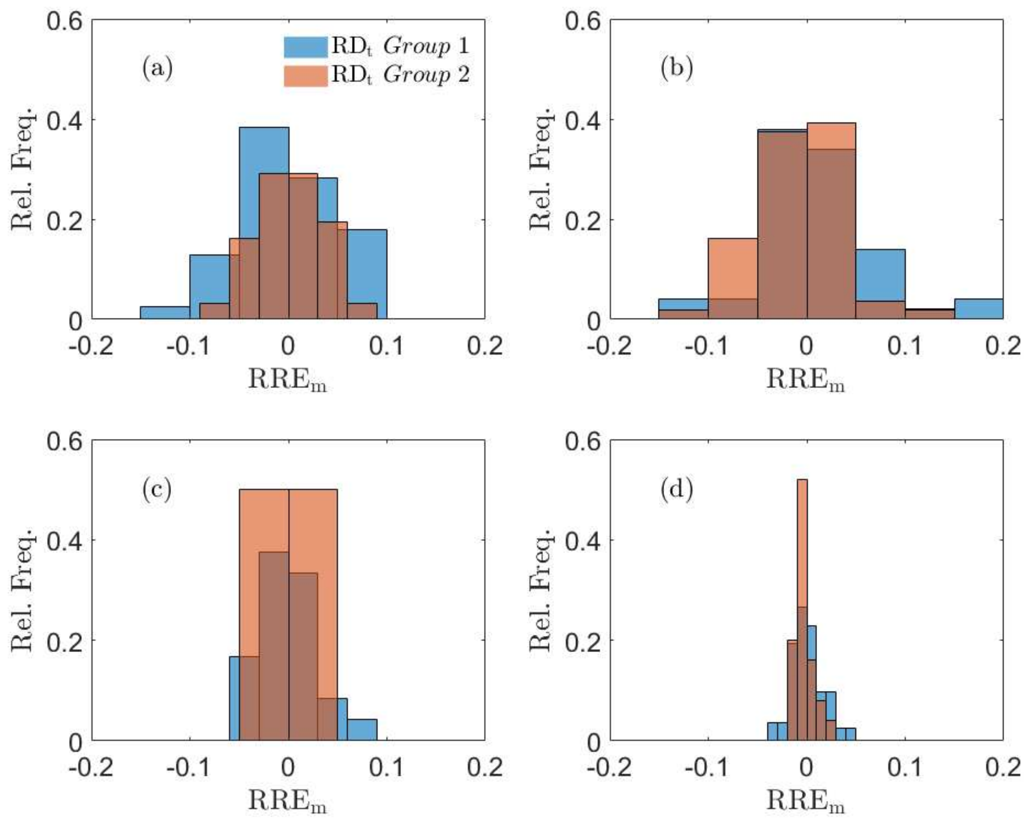

Figure 3.7: Relative frequency histograms of RRE_m, separated by data below the recommended minimum RD_t of 24s/m (RD_t Group 1), and data above the recommended minimum RD_t (RD_t Group 2) for measurement locations (a) R8C, (b) LCC, (c) LWC1, and (d) LWC2.

The p-values indicate a statistically significant difference (significance level of 5%) in the values of var(RRE_m) for the two groups; namely, var(RRE_m) is higher for RD_t Group 1 than RD_t Group 2 for three of the four measurement locations. It is hypothesized that the high p value for the difference in var(RRE_m) between the two groups at LWC1 is due to a low sample size in RD_t Group 2. The reduction in RSU_m by following a relative duration minimum ranges between 0.42 and 2.52 percentage points, averaging 1.41 percentage points across the four locations. This

Table 3.2: Summary statistics for comparison of relative duration parameter groups. p-values indicate results of an one-tailed F-test of variance between data taken outside the recommended minimum RD_t (RD_t Group 1), and those within it (RD_t Group 2). *See Section 3.4.2 for discussion on location LWC1.

Measurement Location	RD_t Group 1 variance	RD_t Group 2 variance	p	RD_t Group 1 Avg. RSU_m (%)	RD_t Group 2 Avg. RSU_m (%)	Reduction in RSU_m (Percentage points),(%)
R8C	0.0022 (n_{t_g}=39)	0.0011 (n_{t_g}=31)	0.0215	5.01	3.28	1.73 (35%)
LCC	0.0036 (n_{t_g}=50)	0.0020 (n_{t_g}=56)	0.0174	6.92	4.40	2.52 (36%)
LWC1	0.0009 (n_{t_g}=24)	0.0005 (n_{t_g}=4)*	0.3326	3.38	2.42	0.96 (28%)
LWC2	0.0003 (n_{t_g}=83)	0.0001 (n_{t_g}=25)	0.0079	1.77	1.35	0.42 (24%)
AVG.						**1.41 (31%)**

suggests that adherence to the recommended guidelines for minimum relative duration of 24 s/m width (7.3 s/ft) per transect yields a significant reduction in uncertainty associated with boat speed protocol.

3.4.3 Number of transects per experiment

Figure 3.8 shows plots of median values of E_s based on N_t, for the four locations. A considerable reduction in Es is observed when four transects are measured instead of only two, and a similar reduction can be seen when six transects rather than four are collected. At locations R8C and LCC, it appears that no considerable reduction in E_s is achieved when using eight rather than six transects. Results of the one-tailed two-sample Wilcoxon rank sum test are shown in Table 3.3. Significant results were achieved at the 5% or 10% significance level for two of four measurement locations when testing if the median E_s when N_t = 4 was smaller than when N_t = 2. Similarly, significant differences at two of three measurement locations were observed when comparing reduction in median E_s when moving from N_t = 4 to N_t = 6.

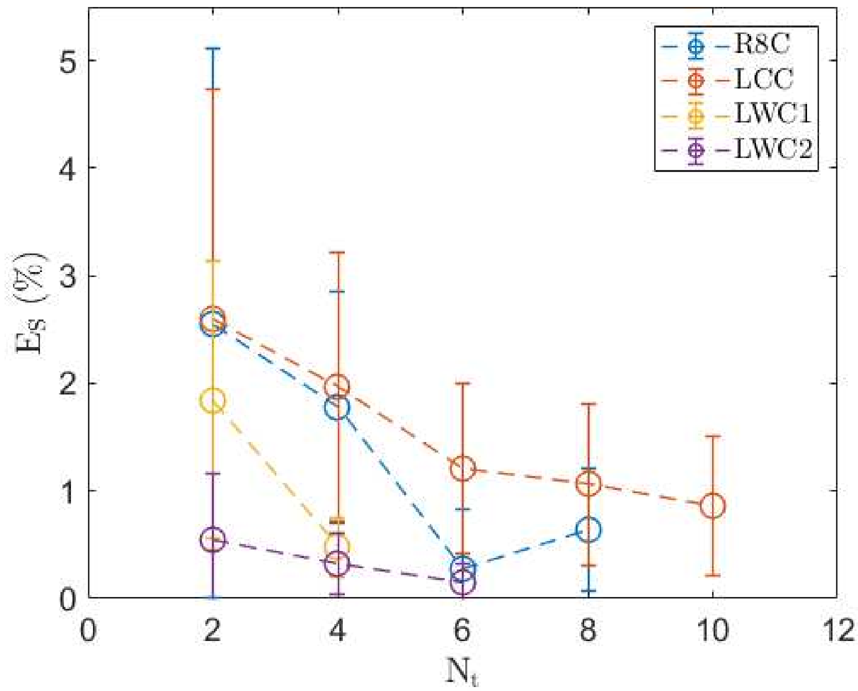

Figure 3.8: Plot of E_s statistics at each measurement location as a function of N_t. Data points indicate median E_s and whiskers indicate median E_s plus or minus one standard deviation.

Table 3.3: Summary statistics for the median values of E_s for each N_t group. p-values shown are the result of a one-tailed two-sample Wilcoxon rank sums test, computing if the median E_s for the given N_t group is significantly less than the median E_s for the next lowest N_t group. Reduction in median E_s is calculated to compare when N_t = 6 (except for LWC1 where N_t = 4) to the median E_s when N_t = 2.

Measurement Location	N_t=2 median E_s (%)	N_t=4 median E_s (%)	N_t=6 median E_s (%)	N_t=4 p	N_t=6 p	Reduction in median E_s (Percentage Points),(%)
R8C	2.56 (n_{s_g}=7)	1.78 (n_{s_g}=7)	0.28 (n_{s_g}=7)	0.268	0.006	2.28 (89%)
LCC	2.59 (n_{s_g}=12)	1.97 (n_{s_g}=11)	1.20 (n_{s_g}=7)	0.240	0.164	1.39 (53%)
LWC1	1.85 (n_{s_g}=4)	0.48 (n_{s_g}=4)	NA	0.014	NA	1.37 (74%)
LWC2	0.538 (n_{s_g}=14)	0.322 (n_{s_g}=13)	0.157 (n_{s_g}=13)	0.069	0.109	0.38 (71%)
AVG.						**1.35 (72%)**

Reduction in median E_s when computing $\overline{Q_m}$ using six transects (or in the case of LWC1, four transects) rather than two transects ranged from 0.38 to 2.28 percentage points, with an average reduction of 1.35 percentage points across the four measurement locations. This suggests that using at least six transects (three pairs of transects taken in reciprocal directions) when measuring discharge using an ADCP will result in a significant reduction in the error of estimating the sample mean.

3.5 Discussion

The findings of this study are dependent on the use of a remotely operated tagline deployment system for traversing the ADCP boat across the canal transect. Figure 3.4 and Figure 3.5 reveal that the unsteadiness of boat movement inherent in the manually-operated rope-and-pulley system confounds any reduction in uncertainty that may be gained by increasing RD_t. Therefore, to reduce uncertainty in ADCP associated with measurement approaches and protocols, remotely operated tagline deployment with more steadiness in boat movement is necessary. If a user is constrained to a manual rope-and-pulley boat deployment method, it is recommended that the protocol guidelines recommended herein are still generally followed, but not sacrificed at the expense of operating the boat at a steady, uniform speed. Results show that RD_t has a significant effect on overall ADCP measurement uncertainty. Dependence of RSU_m on RD_t varies somewhat from site to site; however, it seems clear that refining the current protocol to focus on measurement time per unit width of canal is worthwhile. All experiments were carried out within the constraints of existing guidelines, with sampling times for mean discharge measurement ranging from 726 s to 3900 s. Even so, significant reductions in RSU_m were observed at three of four measurement locations. This indicates a refinement to guidelines in the current literature by indicating that opportunities for mitigating uncertainty are still available when sampling time is > 720 s [49].

An almost exponential decay in RSU_m with increasing RD_t is apparent for the larger canals LWC1 and LWC2. For the smaller canals, LCC and R8C, the decrease is more linear. The exponential trend is expected based upon standard analyses of uncertainty and measurement duration [37].

It was the goal of this study to identity a point of diminishing returns for ADCP transect duration, i.e. to find the minimum value of RD_t beyond which uncertainty is likely not to change much. Although data for all measurement locations did not fall cleanly along the same trend due to differences in favorability for measurement between locations, results suggest that a minimum RD_t of 24 s/m (7.3 s/ft) is a conservative place to start when making ADCP measurements. Users are encouraged to increase RD_t under unfavorable field conditions. For example, at site LCC where there was excessive bank vegetation, mild curvature in the canal path, and an excessive extension of the portion of the flow width that was not directly measurable at higher flow rates, flow measurement was relatively more difficult. A more reasonable recommendation of RD_t for this site may be 30 s/m (9.1 s/ft). However, as can be seen in the results (Table 2), the guideline of 24 m/s (7.3 s/ft) still decreased RSU_m by about 36% (2.52 percentage points).

The value of N_t to use for an ADCP deployment is also an important, though less crucial, element of measurement protocol [11]. Results in Figure 3.8 and Table 3.3 show that significant reductions in the relative difference of the sample mean to the estimated population mean are likely when including four or six transects to compute $\overline{Q_m}$ rather than only two, as is the current popular practice. Under the assumption of measurement of steady flow in irrigation canals, we conservatively recommend that at a minimum six transects be collected to determine mean discharge. Collecting more than six transects may slightly reduce uncertainty but this improvement is not likely to be significant, as can be seen from Figure 3.8.

Finally, it is apparent that the choice of measurement location along a canal is a critical factor influencing uncertainty. Patterns from comparing relative levels of uncertainty with site characteristics indicate that both the percentage of total discharge that is directly measured as Q_m by the ADCP, as well as the cross-sectional area of the flow, seem to be negatively correlated with RSU_m. Alternatively stated, gauging flow in smaller canals is often correlated with more unfavorable measurement conditions. Special scrutiny of measurement site selection should be made to follow the guidelines listed above. This includes giving attention to the limitation of the amount of bed and bank vegetation, curvature in canal path, surface waves, exposure to wind, and the amount of large boulders on the canal bed. Surface waves caused by a supercritical regime, along with highly turbulent flow, should also be avoided. In general, these guidelines agree with the USGS that the user "limit the portion of unmeasured flow area as much as possible" [11].

3.6 Conclusions

Boat-mounted ADCPs are widely used to measure open-channel flows; however, currently there are no clear guidelines on how fast to move the boat when completing one transect across the channel, nor on the total number of transects to use in computing average discharge. Results of multiple field experiments carried out at four locations in small to moderate-capacity canals suggest a protocol of multiplying the width of the ADCP transect across the canal measurement location by a minimum relative duration of 24 s/m (7.3 s/ft) to obtain the duration for a single transect and using a minimum of six transects to compute the average discharge of steady flow. However, it should be noted that this guideline for relative transect duration assumes measurement using a *StreamPro* ADCP with vertical pings taken at a rate of 1 Hz. As an aspect of future study, there is potential to examine the robustness and scalability of our minimum recommended value for this parameter using moving-boat ADCPs with higher sampling rates. Separately, choosing a system of boat deployment that ensures stability and a steady speed, along with careful selection of measurement location, is also recommended.

Results reveal that following these protocols may reduce uncertainty metrics in overall discharge quantification by an average of about 30 to 70%, potentially leading to sizeable economic consequences. For an exemplary worst-case scenario, the reduction by 1.4 percentage points in the uncertainty metric associated with transect relative duration alone, if applied to an average flowrate of 7 m^3/s (typical for a mid-sized irrigation canal in the Larimer and Weld Irrigation District) operating over a 200-day irrigation season could result in the improved accounting of approximately 1.69 MCM (1371 ac-ft) of water. Applying a conservative estimate of US$8.10/$m^3$ (US$10,000/acre-ft) to this volume of water within Colorado's South Platte River Basin [55], these protocols could result in a potential annual savings of about US$14 million. Additionally, these recommended protocols will aid in the calibration of hydraulic structures within canals, allowing rating curves to be established with a greater degree of accuracy and reliability.

The information provided herein does not supersede the established wealth of knowledge regarding best practices for performing reliable and accurate discharge measurements using an ADCP. The literature points to numerous interacting sources of uncertainty in ADCP measurement, beyond those considered here, that are worthy of diligent examination. Rather, we provide a closer scrutiny of a few user-dependent measurement protocols which indicate a potential for reduction in uncertainty metrics.

The authors offer the results of this study as an aid in refining current best-practice literature on ADCP flow measurement with a special consideration to irrigation water management. We refer the reader to other helpful guidance documents on moving-boat ADCP measurement within a broader context, and on hydro-acoustics in general [11, 29, 37, 42, 48, 52, 56]. There exists future potential to expand the relevance of these findings by studying larger channels using a suite of commonly-used ADCPs, along with the prospect to further refine the guidance established by the exploratory nature of the present study.

More accurate quantification and more just allocation of our increasingly limited water resources is essential for the prudent stewardship of this precious natural resource. The authors are hopeful that promoting the recommendations contained herein for the reduction of uncertainty in measuring flows in small-to-moderate irrigation canals will serve as valuable tool for water resource engineers and managers toward this end.

Chapter 4

Investigating the Nature of the Obermeyer Pivot Weir Rating Equation

4.1 Introduction

As discussed in Section 2.3, the Obermeyer pivot weir represents a novel method for controlling water stage levels in irrigation canals. However, currently there does not exist any substantial published literature on the nature of the stage-discharge relationship for this particular structure. The Obermeyer invention is a specialized type of pivot weir that differs primarily from other structures of this general type in that the gate leaf of the weir is cambered, and the crest elevation is controlled by a series of inflatable air bladders. Previous studies in the literature have examined the stage-discharge relationship for a thin flat plate pivot weir that resembles a sharp-crested weir tilted at an angle to the horizontal. The most widely accepted approach taken to develop a rating curve for the pivot weir, published by Wahlin and Replogle (1994) [20], has been to introduce an additional discharge coefficient that is a function of the inclination angle, θ. However, the acceptability of this approach to pivot weirs of a specialized geometry, such as the Obermeyer design, remains undetermined due to the empirical nature of developing calibration coefficients for the inclination angle. Where it can be achieved, a more theoretical basis for establishing a rating equation should be pursued, due to uncertainty in reliability of empirical calibration arising from variability in the methodological approaches taken by experimentalists.

In light of this, the current study investigates the possibility of reducing the dependability of the Obermeyer rating equation on empirical calibration by pursuing a more theoretical approach of accounting for the effect of the changing inclination angle on the flow dynamics. This is done by reanalyzing some of the basic assumptions implicit in the sharp-crested weir rating equation. Section 2.3.1 lists these in full, but two major assumptions examined for pivot weirs in the current study are: the neglect of the upstream velocity head in the Bernoulli conservation of energy equation, and the assumption of no frictional energy losses (i.e. inviscid or ideal flow) between the upstream location where the elevation head is measured, and the crest. If one is to first allow for the assumption of inviscid flow, the effect of the changing inclination angle, θ, on the flow dynamics can be hypothesised. Reduction in the inclination angle from the 90°sharp-crested weir case would result in less impedance to the flow, allowing for less deceleration in the upstream velocity field. Hence, the overall contribution of the velocity head to the total upstream mechanical energy head, given by Eq. (2.5), would increase as the inclination angle decreases. An alternative way to summarize this effect is that for a constant discharge, Q, the elevation head above the crest, h decreases as the angle of inclination, θ decreases, while H is still conserved due to increasing flow velocity. Thus, in theory the effect of the changing inclination angle on the pivot weir rating equation could simply be achieved by accounting for the total upstream mechanical energy head (i.e. no longer neglecting the velocity head), and no additional discharge coefficient is needed. The formation of this hypothesis was informed by analysis of data provided by Wahlin and Replogle (1994) in their laboratory study of pivot weirs. These data, shown in Figure 4.1 reveal a clear trend between the inclination angle, θ, and the percentage contribution of the velocity head to the total mechanical energy head. Hence, the accuracy of proposing an analysis of the total mechanical head as sufficient to explain the effect of the inclination angle in the pivot weir rating equation is investigated in the current study.

With this new proposed approach, and the other potential alternatives present in the literature for establishing a pivot weir rating equation, it is still yet to be seen which is most applicable to the case of the Obermeyer weir. Also, to the knowledge of the author, no study has been completed thus far based upon the observation of pivot weirs at an operational field scale. Wahlin and Replogle (1994) collected a small set of field observations on two different structures in the Imperial Irrigation District of Southern California. However, the scale of these structures remained moderately small and on par with laboratory models, with maximum discharge $\leq$ 31.09 cfs [20]. The current study consists of observations on a major irrigation conveyance canal with an approximate

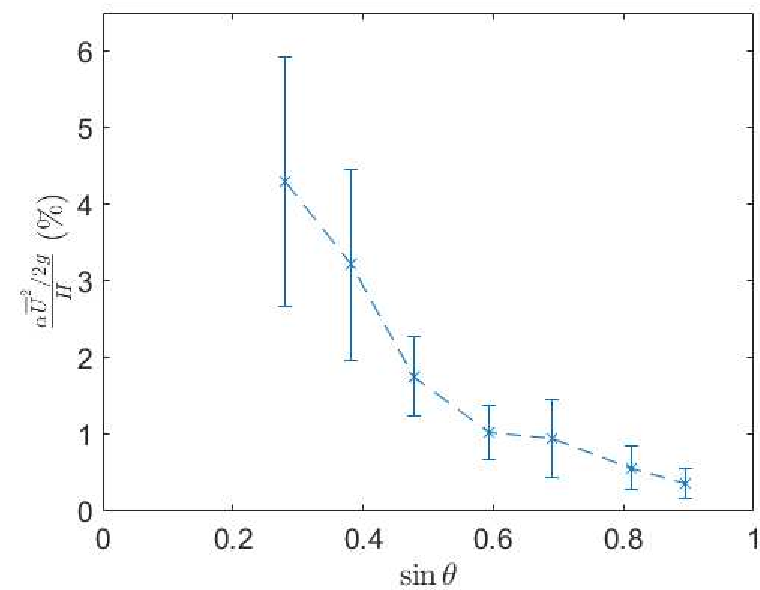

Figure 4.1: The results of 125 observations on the Armtec gate published by [20], plotted to show the percent contribution of the kinetic energy head to the overall total mechanical energy head as a function of the weir inclination angle. Error bars represent $\pm$ one standard deviation.

top width of 39 ft (11.9 m) and average discharge of 221 cfs (6.3 m^3/s), representing a typical functional scale for pivot weirs used for irrigation water management. Observing the structures at an operational scale allows for a check against findings made in the laboratory.

Hence, several aspects pertaining to the development of a stage-discharge relationship for the Obermeyer pivot weir remain open questions. These are the questions the current emerging work attempts to investigate:

- Can the effect of the changing inclination angle, θ, on the flow dynamics be sufficiently explained when the total mechanical energy head is incorporated into the pivot weir rating equation? If so, how practical is it to gain an accurate estimation of the velocity head?

- If, however, the upstream velocity head is neglected and effect of the gate angle on the flow must be incorporated in to the rating equation via an additional empirically-derived discharge coefficient, how applicable is this formula to weirs of differing geometries, scales, and settings?

- What is the relative importance of the the changing inclination angle and varying h/p ratio on the discharge coefficient? Is one more important to consider than the other? Alternatively, is C_d independent of h/p within a certain operational range? If so, how does this range of h/p shift with θ?

- Is there good agreement between the field observations of functional Obermeyer pivot weirs and measurements from previous studies made on scaled laboratory models of generalized pivot weirs?

- What are the practical limitations for accurately developing a pivot weir rating equation that must be considered?

4.2 Field measurements along Larimer and Weld Canal

A major campaign to establish a robust set of field observations of Obermeyer pivot weirs was lead by previous CSU M.S. student Caner Kutlu from 2017-2018 [57]. During this study, 96 unique paired observations of stage, discharge, and inclination angle were collected at three different Obermeyer pivot weir structures along the Larimer and Weld irrigation canal in Weld County, Colorado. The author of the current work added a supplementary 12 observations at a single structure to the existing field data set during the summer of 2020. A summary of field observations on Obermeyer pivot weirs is provided in Table 4.1. In total, 108 observations were collected. Measurement of steady mean discharge was determined using an ADCP at a cross-section located approximately 7 m upstream from the weir crest. The depth cell sizes ranged from 8-9 cm. The total measurement time was at least 720s for all computations of discharge, typically taken over four transects. The average RSU (%) for a single transect was 2.44 % across all observations [58].

In the current study, stage measurements were conducted using a staff gauge that was affixed to the concrete retaining wall of Gate A, approximately 7 m upstream from the crest. A surveying tripod and auto-level were used to carefully record the water surface elevation from the opposite

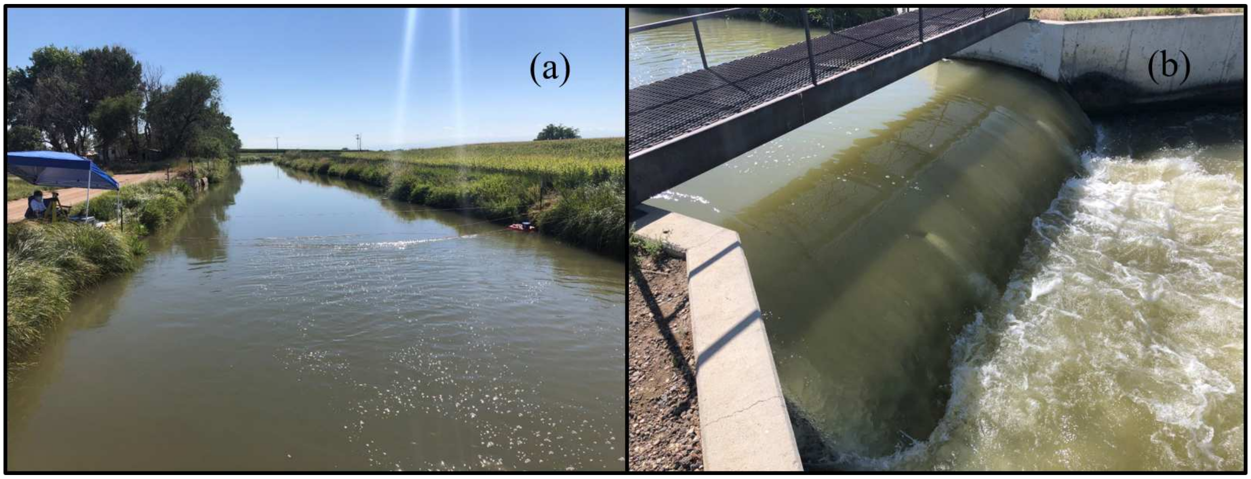

Figure 4.2: Site photos of Gate A measurement section: (a) ADCP measuring discharge upstream of structure, and (b) Weir flow over Gate A crest at a moderate flow rate. Notice design elements of diverging side walls and nappe breakers along the weir crest which allow for atmospheric pressure underneath the nappe.

bank. The flow within the canal was remarkably steady for the duration of the measurements. Record of the stage was made every five minutes to ensure no drastic changes in the upstream energy condition. Additionally, computation of the velocity head was possible using data gathered with the ADCP. Hence, the total mechanical energy head upstream of Gate A could be calculated and incorporated into the stage-discharge equation.

The angle of the pivot weir to the horizontal was determined in a step-wise manner. First, at the time of flow quantification only a horizontal measurement of the weir crest location in relation to a fixed reference point along the top of the retaining wall was available (see Figure 4.2).

Table 4.1: Summary of field observations of Obermeyer pivot weirs taken along the Larimer and Weld Canal. Observations in bold were measured by the current author. All other data is courtesy of Caner Kutlu (2019).

					Number of Observations		
Gate	Crest length - b (m)	Gate Length - L_g (m)	Range for θ	Range for Q (m^3/s)	2017	2018	2020
A	6.73	1.74	19.1°-29.8°	2.16-9.38	22	19	***12***
B	6.11	2.10	31.9°-36.3°	2.20-8.70	16	18	NA
C	5.20	2.20	20.8°-28.3°	4.91-7.54	21	NA	NA

Vertical measurement of the weir crest height was not possible due to the high amount of flow within channel during measurement. This required an additional trip to the field locations after the irrigation season was over and the canals were drained. At this time, the location of the crest was reset to the specific location which occurred on the day of measurement, as determined by the earlier horizontal reference measurement. The height of the weir crest, p, was then measured, and θ determined as: $\theta = \arcsin{(p/L_g)}[radians]$.

4.3 Stage-discharge relationship from field data: alternative approaches

Four distinct approaches were taken to develop a stage-discharge relationship and estimate the discharge coefficient for the Obermeyer pivot weir based on the collected field data. The general process of Bijankhan and Ferro (2018) [22] was used, where the value of the discharge coefficient is determined using least-squares linear regression. The curve-fitting tool in MATLAB (v2020a) was used for all linear and non-linear regression analysis. However, the approaches varied in the incorporation of the velocity head into the rating equation, and the inclusion of an additional discharge coefficient to account for the effect of a changing inclination angle.

Data from Gates A and B taken by Kutlu (2019) during the 2017-2018 irrigation seasons were used as the base set by which to calibrate the discharge coefficient for the stage-discharge equation. Data from Gate C were excluded from the coefficient calibration in order to examine the applicability of the developed rating equation to a structure with slightly different geometric aspect ratios. 2020 data taken at Gate A were also excluded from the calibration and allowed an independent check on the reproducibility of the stage and discharge measurement protocols described in Section 4.2.

4.3.1 Approach 1: $\mathbf{C_d = f(h)}$

The first approach is essentially a directly modified version of the classical sharp-crested weir rating equation (2.10). Here, the upstream velocity head is neglected and no additional discharge coefficient is included to account for changes in the inclination angle. It is assumed that within the operational range of inclination angles for the pivot weir, being $19.1° \leq \theta \leq 36.3°$ in the current study, that the discharge coefficient will remain relatively constant. With C_d only being a function of the elevation head, the effect of varying h/p values on the discharge coefficient is also neglected. This approach represents the simplest of all possible alternatives examined in this study because it does not require estimation of either the velocity head or the inclination angle of the pivot weir. It was not expected to perform well against the other alternatives and represents a base case against which other alternative approaches can be compared. The rating equation associated with this approach is written as:

$$Q = \frac{2}{3} C_{d_{f-h}} \sqrt{2g} b {h_1}^{3/2}; \tag{4.1}$$

where the discharge coefficient is written as $C_{d_{f-h}}$ to reflect that it is a fixed value determined using only the elevation head, h. The value of $C_{d_{f-h}}$ was determined by plotting all 75 observations of the calibration set from Kutlu (2019) and performing a linear regression with forced zero intercept to determined the value of the coefficient a in Eq. (2.16). The exponent m was assumed to be unity in accordance with the recommendation from Bijankhan and Ferro (2018) [22]. Then, the best fit value of a was transformed using Eq. (2.18) into the standard C_d as it appears in Eq. (2.10).

Figure 4.3 shows the regression analysis to estimate the value of $C_{d_{f-h}}$, with $a = 0.7113$. It can be seen that the fit is fairly linear but that the observed data deviates from the line of best fit near the extreme ranges of h/p. Most notably, a potential lower limit for h/p of approximately 0.5 can be observed, where the linear fit begins to deviate strongly from the observed data. Using Eq. (2.18), the discharge coefficient for Eq. (4.1) can be defined as:

$$C_{d_{f-h}} = 0.636. \tag{4.2}$$

.

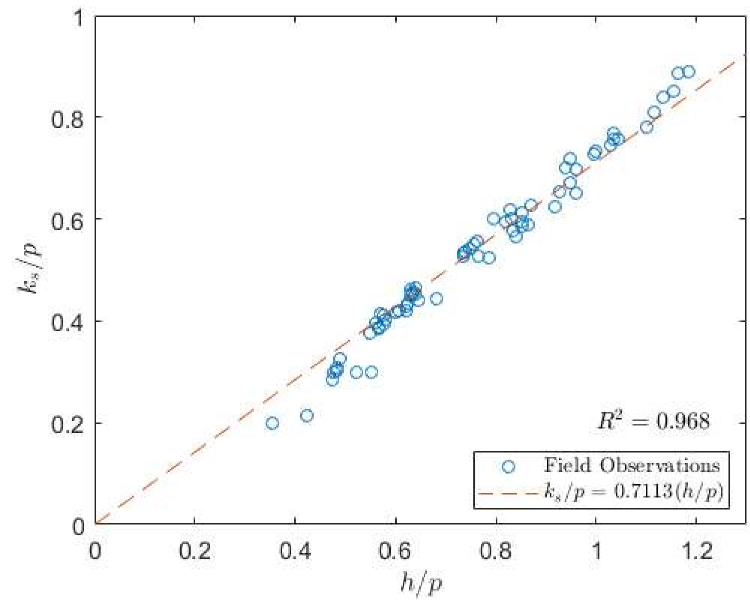

Figure 4.3: Plot of k_s/p vs. h/p for calibration of the discharge coefficient under approach 1 as a fixed value independent θ, h/p.

4.3.2 Approach 2: $\mathbf{C_d = f(H)}$

The second approach allows for the consideration of the upstream velocity head in to the Bernoulli equation (2.4), and assumes a fixed discharge coefficient. This approach represents the examination of the hypothesis laid out in Section 4.1, where the effect of the changing inclination angle essentially represents a redistribution of the respective contributions of the elevation head and velocity head to the overall total mechanical energy head, H. Thus, if the rating equation is allowed to be a function of H, it is assumed that an additional discharge coefficient to account for the inclination angle is unnecessary if viscous effects within the flow can be safely neglected. Here, H is defined as:

$$H = h + \alpha\frac{\overline{U}^2}{2g}; \tag{4.3}$$

where the datum for the elevation head is assumed to be the crest elevation. α, defined by Eq. (2.6) was determined using ADCP data, with $\int u^3 A$ taken to be the integral of all respective cubed stream-wise velocity calculations for each bin (cell) measured by the ADCP, multiplied by the the bin area. $\overline{U}$ was determined as the mean of all u, and A was the total flow area as determined by the ADCP. An average value of α = 1.1 was used in accordance with the analysis done by Kutlu (2019).

This approach relies more upon theoretical reasoning rather than empirical calibration and thus represents a potentially more elegant solution to developing a pivot weir rating equation. The pivot weir rating equation for approach 2 takes the form:

$$Q = \frac{2}{3} C_{d_{f-H}} \sqrt{2g} b {H_1}^{3/2}. \tag{4.4}$$

The calibration for an estimated value of $C_{d_{f-H}}$ was done a similar manner to approach 1. Figure 4.4 shows that a was estimated as 0.6991, yielding a discharge coefficient of:

$$C_{d_{f-H}} = 0.620. \tag{4.5}$$

The linear fit in Figure 4.4 is revealed to be only nominally better than the fit in Figure 4.3, exhibiting similar poor performance at the lower range for H/p. Approach 2 represents a slightly more complex method compared to approach 1 because it takes into account the contribution of the upstream velocity head into the rating equation. Therefore, this approach is potentially less practical to implement because an estimation of the upstream velocity head is typically difficult to estimate without a direct flow measuring device such as an ADCP. Alternatively, a hydrographer would have to rely on an empirical relationship between the stage, h and the velocity head $\alpha \overline{U}^2/2g$ to estimate the total mechanical energy head, H.

4.3.3 Approach 3: $\mathbf{C_d = f(h, \theta)}$

Due to the practical difficulty of estimating the upstream velocity head, the effect of the changing inclination angle on the overall rating equation instead can be quantified using an additional empirically-derived discharge coefficient. This is the approach that has thus far been implemented by past authors Wahlin and Replogle (1994) and Bijankhan and Ferro (2018). It essentially accounts for the increased contribution of the velocity head into the energy equation as the inclination

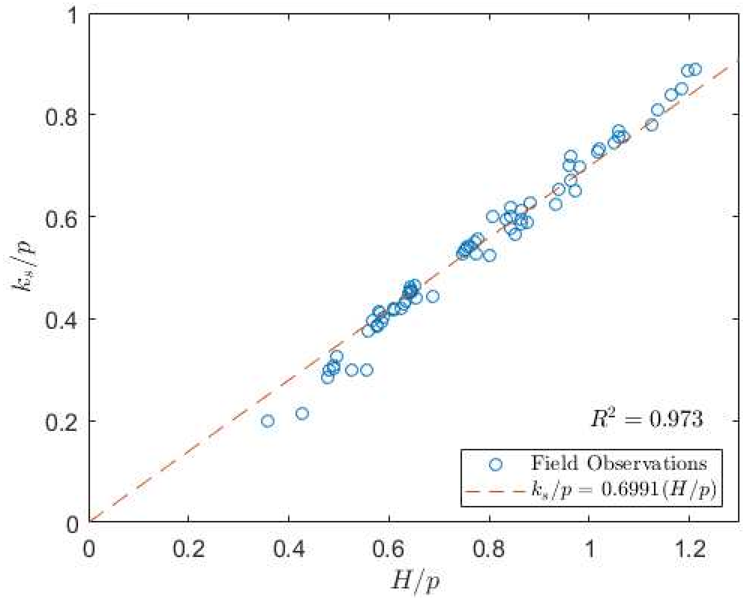

Figure 4.4: Plot of k_s/p vs. h/p for calibration of the discharge coefficient for approach 1 as a fixed value independent of θ.

angle decreases, but neglects the variability in the discharge coefficient with h/p, especially at low inclination angles. It takes the form:

$$Q = \frac{2}{3} C_{d_{\theta-h}} \sqrt{2g} b {h_1}^{3/2}. \tag{4.6}$$

Here, $C_{d_{\theta-h}}$ is a power function dependent on the sine of the inclination angle. Eq. (4.6) represents a very similar approach to that of (2.11) in the Wahlin and Replogle (1994) study. However, whereas an effective discharge coefficient is used in Eq. (2.11) that is a modified form of the generalized Rehbock equation, $C_{d_{\theta-h}}$ in (4.6) of the current study is calibrated specifically to the structures in the present study and is thus expected to be more accurate than the Rehbock equation (2.12).

Calibration of $C_{d_{\theta-h}}$ was done by estimating the linear slope coefficient, a, of (2.16) for groups of observations taken at the same inclination angle, for the range $20.51^\circ \leq \theta \leq 36.31^\circ$. Figure Figure 4.5 shows the results of this process. Similar to the procedures in approaches 1 and 2, the coefficient a was then transformed to the standard discharge coefficient form, and an estimated discharge coefficient was determined for each inclination angle value, shown in Figure 4.5.

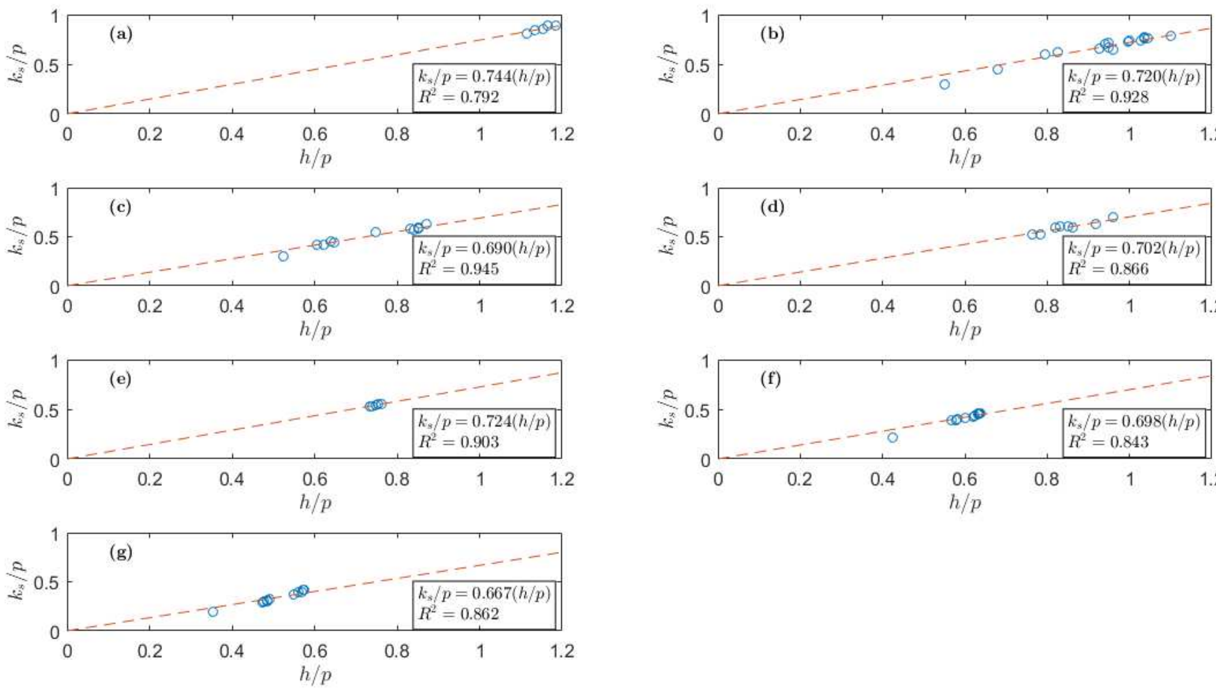

Figure 4.5: Results of regression analysis to calibrate value of discharge coefficient as a function of gate inclination angle, for values of: (a) 20.51°; (b) 25.75°; (c) 28.11°; (d) 29.83°; (e) 31.89°; (f) 35.08°; (g) 36.31°

Then, a non-linear regression was performed to fit a curve to these values as a function of $\sin\theta$. A power curve fit was chosen under the assumption that the effect of the gate angle on the discharge coefficient would asymptotically decrease as θ approaches 90°. The curve was fit as a function of $\sin\theta$ to avoid potential confusion amongst future readers as to whether θ should be written in degrees or radians. This approach also allows one to easily visualize an approximation of what the lower limit of C_d is when the gate becomes a vertical sharp-crested weir at $\sin\theta = 1$. The fit of this regression line to the data is shown in Figure 4.6, and the results of this curve-fitting are given by (4.7).

$$C_{d_{\theta-h}} = 0.535(\sin\theta)^{-0.225}. \tag{4.7}$$

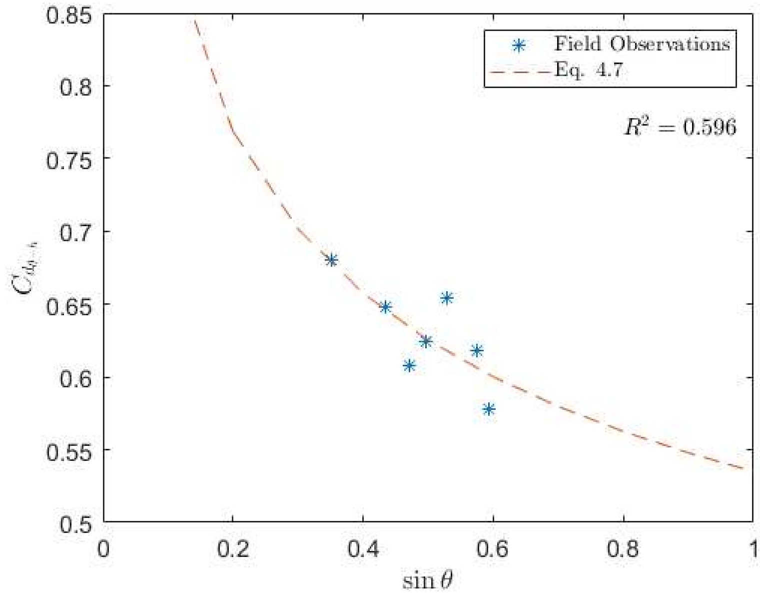

Figure 4.6: Plot of $C_{d_{\theta-h}}$ curve given by Eq. (4.7) against estimated $C_{d_{\theta-h}}$ values from field observations.

Although (4.7) estimates the lower limit of the discharge coefficient to be $C_{d_{\theta-h}} = 0.535$ when $\theta = 90°$, the true behavior of the discharge coefficient should not be extrapolated beyond the range of inclination angles from which (4.7) was derived: $19.1° \leq \theta \leq 36.3°$. In fact, data presented by Bijankhan and Ferro (2018) suggest that $C_{d_{\theta-h}}$ may even increase as θ approaches 90°. Hence, the question of whether the relationship between the discharge coefficient and the inclination angle as θ approaches 90°remains truly monotonic is a topic of continued research.

It can be seen that the fit of (4.7) to the observed field data is not excellent ($R^2 = 0.596$). One potential reason for this is the inherent uncertainty in field measurement of the key parameters of stage level, discharge via ADCP, and weir inclination angle. Although the respective uncertainty in a single one of these measurements may be brought within an acceptable range (as expounded upon in Chapter 3), a compounding effect occurs when the uncertainties of each of these measurements is compiled in the development of a discharge rating equation, such as Eqns. (4.6) and (4.7). For this reason, this calibration should be noted as a fairly good representation of the flow dynamics occurring in the field, but that opportunity exists for further elucidation using laboratory methods subject to lower relative levels of inherent measurement uncertainty.

Similar to approach 2, approach 3 represents a more complex rating equation than (4.1) in approach 1. It requires the ability to measure the weir inclination angle in the field, which is a matter of practical difficulty. For the use of this approach, some mechanism for measuring θ while flow is actively passing through the canal must be installed for the structure. Hence, the overhead costs may be large. Furthermore, for a given value of θ, approach 3 assumes that the discharge coefficient, $C_{d_{\theta-h}}$ will remain constant irrespective of changing h/p values. This is known to be a fairly acceptable assumption for the case of the sharp-crested weir when the flow velocity is small and elevation head is large, making contribution of the velocity head to the total head, H, small. However, as θ decreases, the percentage make-up of the velocity head to the total head will increase, rendering the assumption to neglect the upstream velocity head a worse and worse simplifying assumption.

4.3.4 Approach 4: $\mathbf{C_d = f(H, \theta)}$

For this reason, a fourth approach to developing a rating equation for the Obermeyer pivot weir is investigated, where the discharge coefficient is both a factor of a inclination angle measurement, as well as the total mechanical energy head. This represents a combination of approaches 2 and 3, and all terms and methods of calibration are consistent with those mentioned in the preceding sections. The rating equation for this approach takes the form:

$$Q = \frac{2}{3} C_{d_{\theta-H}} \sqrt{2g} b {H_1}^{3/2}. \tag{4.8}$$

The calibration for discharge coefficient estimation with respect to the inclination angle is shown in Figure 4.7, with the power-curve fit that gives the predicted value of $C_{d_{\theta-H}}$ as a function of $\sin\theta$ shown in Figure 4.8 and given by Eq. (4.9):

$$C_{d_{\theta-H}} = 0.533(\sin\theta)^{-0.196}. \tag{4.9}$$

This fourth approach represents the most complex and empirically dependent equation of the alternatives examined so far. It requires not only knowledge of the inclination angle, but also the upstream velocity head so that the total mechanical energy head can be computed. It is likely to be the most accurate approach of the alternatives investigated because it accounts for changes to the flow dynamics via the changing inclination angle, as well as variations in h/p (i.e. the stage level passing over the weir). However, it implies the practical limitation of obtaining an estimation of the inclination angle and velocity head.

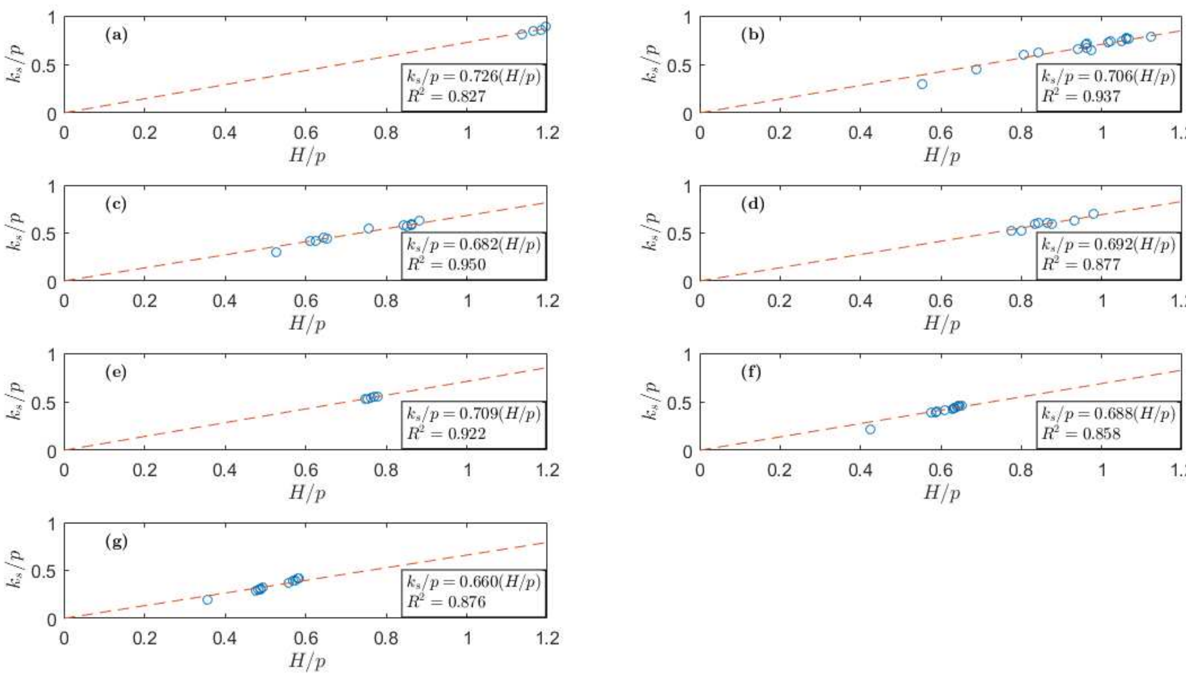

Figure 4.7: Results of regression analysis to calibrate value of discharge coefficient as a function of gate inclination angle and total head (H), for values of: (a) 20.51°; (b) 25.75°; (c) 28.11°; (d) 29.83°; (e) 31.89°; (f) 35.08°; (g) 36.31°

To elucidate which of these approaches represents an optimal balance between desired accuracy and practicality for implementation, an error analysis was conducted. For the purpose of clarity, the four alternative rating equation approaches discussed in the preceding sections are summarized here in their full form with functions for the discharge coefficient inserted directly into the equation.

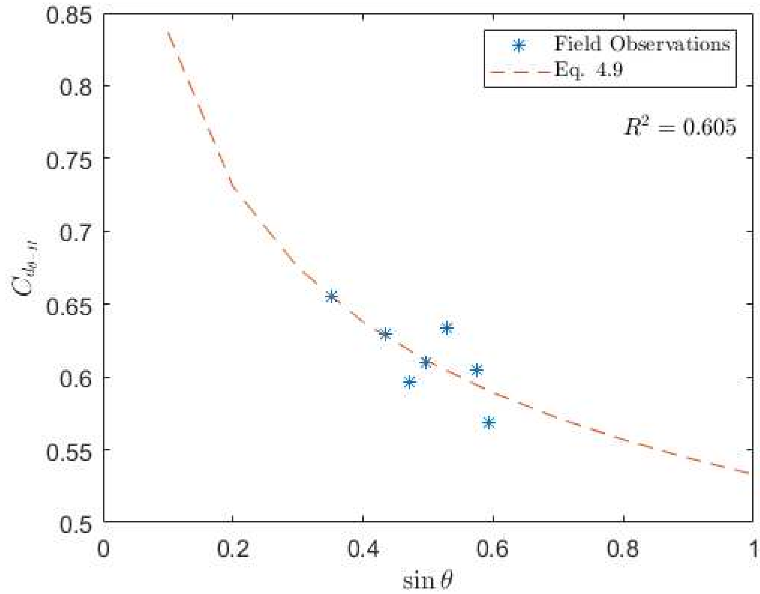

Figure 4.8: Plot of $C_{d_{\theta-H}}$ curve given by Eq. (4.9) against estimated $C_{d_{\theta-H}}$ values from field observations.

They are listed in ascending order according to the associated approach number.

$$Q = \frac{2}{3}[0.636]\sqrt{2g}bh_1{}^{3/2} \tag{4.10}$$

$$Q = \frac{2}{3}[0.620]\sqrt{2g}bH_1{}^{3/2} \tag{4.11}$$

$$Q = \frac{2}{3}[0.535(\sin\theta)^{-0.225}]\sqrt{2g}bh_1{}^{3/2} \tag{4.12}$$

$$Q = \frac{2}{3}[0.533(\sin\theta)^{-0.196}]\sqrt{2g}bH_1{}^{3/2} \tag{4.13}$$

4.4 Performance analysis of approaches

First, as a way to qualitatively examine the performance of each approach, Figure 4.9 and Figure 4.10 show scatter plots of relative error.

These scatter plots reveal that each approach performs fairly well, with the majority of the 108 rating equation discharge predictions falling within $\pm 15\%$ of the ADCP measured discharge. Larger discrepancies from the measured discharge, representative of poor rating equation performance, are seen near the lower range of observed flow rates. Here, the predicted discharge is far

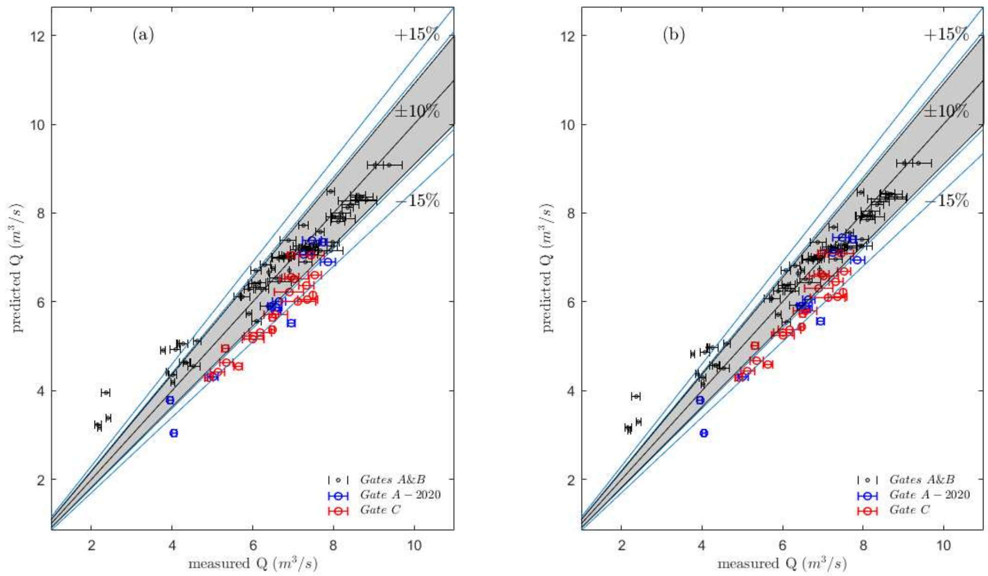

Figure 4.9: Scatter plot of relative error for (a): Eq. (4.10) and (b): Eq. (4.11). 1:1 line of agreement between Q predicted by the rating equations and measured by ADCP is shown as dark bold line. Bands for $\pm 10\%$ displayed as shaded gray area, with limits for $\pm 15\%$ displayed by blue lines. Horizontal error bars represent $\pm\%RSU$ values as an indication of uncertainty in measured ADCP flow rate.

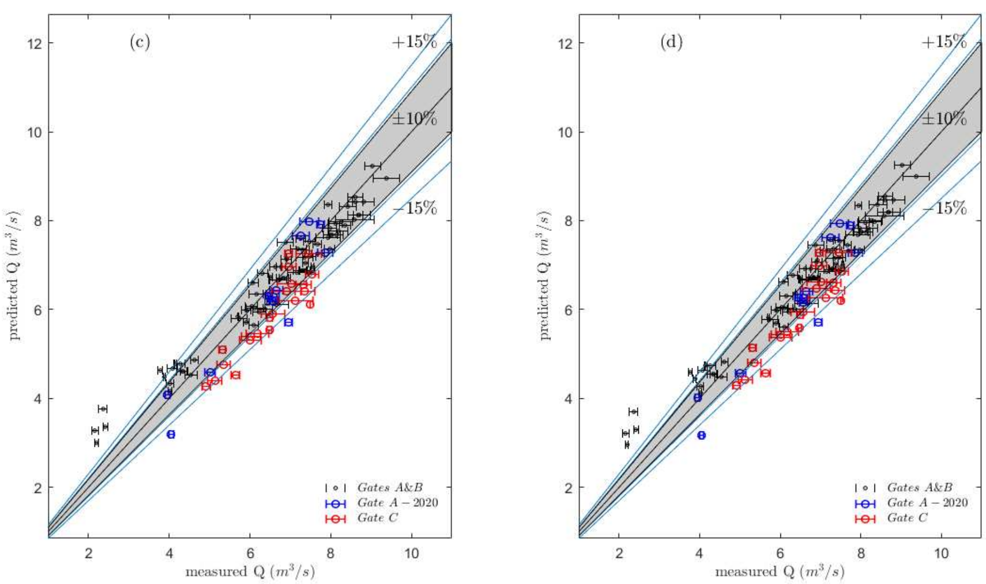

Figure 4.10: Scatter plot of relative error for (c): Eq. (4.12) and (d): Eq. (4.13). 1:1 line of agreement between Q predicted by the rating equations and measured by ADCP is shown as dark bold line. Bands for $\pm 10\%$ displayed as shaded gray area, with limits for $\pm 15\%$ displayed by blue lines. Horizontal error bars represent $\pm\%RSU$ values as an indication of uncertainty in measured ADCP flow rate.

larger than the measured discharge, indicating a large drop-off in the discharge coefficient at low flows. This may be indicative of a lower limit for h/p for the operational range of the Obermeyer pivot weir that merits further investigation. This limit would represent a point were the fundamental dynamics of the flow shift, and the assumptions concerning the ability to neglect viscous and surface tension effects is no longer valid. Figure 4.9 and Figure 4.10 also reveal that each rating equation predicts the large majority of observed discharge points within the calibration set at the $\pm 10\%$ level. Good agreement is also seen within the Gate A - 2020 set, which verifies a sufficient level of reproducibility in these results (see Section 4.3). However, larger discrepancies exist for the validation set of Gate C, where the measured discharge is typically under-predicted. This represents potential evidence for the sensitivity of empirically-calibrated discharge rating equations, where deviations in the aspect ratio of the structure from those examined for calibration may result in inaccurate discharge prediction. For this reason, unique calibrations for each structure should be completed whenever possible.

To further investigate performance differences between the four rating equation approaches investigated, mean squared error (MSE) and mean absolute percent error (MAPE) are analyzed. First, squared error (SE) is the square of the difference between the predicted discharge and the measured ADCP discharge, defined as:

$$SE = (Q_{predicted} - Q_{measured})^2. \tag{4.14}$$

The mean of the squared error values is taken from all 108 observations in the field data set. MSE is chosen as a comparison statistic because squared errors are typically normally distributed, thus simplifying the statistical methods required for analysis. MAPE is another useful statistic which characterizes the average percent difference in the rating equation predicted discharge and the measured discharge.

$$MAPE(\%) = \overline{[\frac{|Q_{predicted} - Q_{measured}|}{Q_{measured}} * 100]}. \tag{4.15}$$

To increase the robustness of statistical comparison between approaches by analyzing confidence intervals within which the true value of MSE is expected to reside, a bootstrapping sampling procedure is completed [59]. This method randomly selects a value within the distribution of squared error values for a particular approach a repeated number of times. For the current study, a bootstrapped sample size of 100,000 was chosen. This sampling was done with replacement, meaning the same unique value within the distribution of squared error could be chosen more than once. The large bootstrapped sample size then allows for visualizing the normal distribution of squared error values around the MSE using frequency histograms, and the computation of confidence intervals for the true value of MSE. Relative frequency histograms for the distribution of squared error associated with each rating approach are shown in Figure 4.11 with summary statistics provided by Table 4.2.

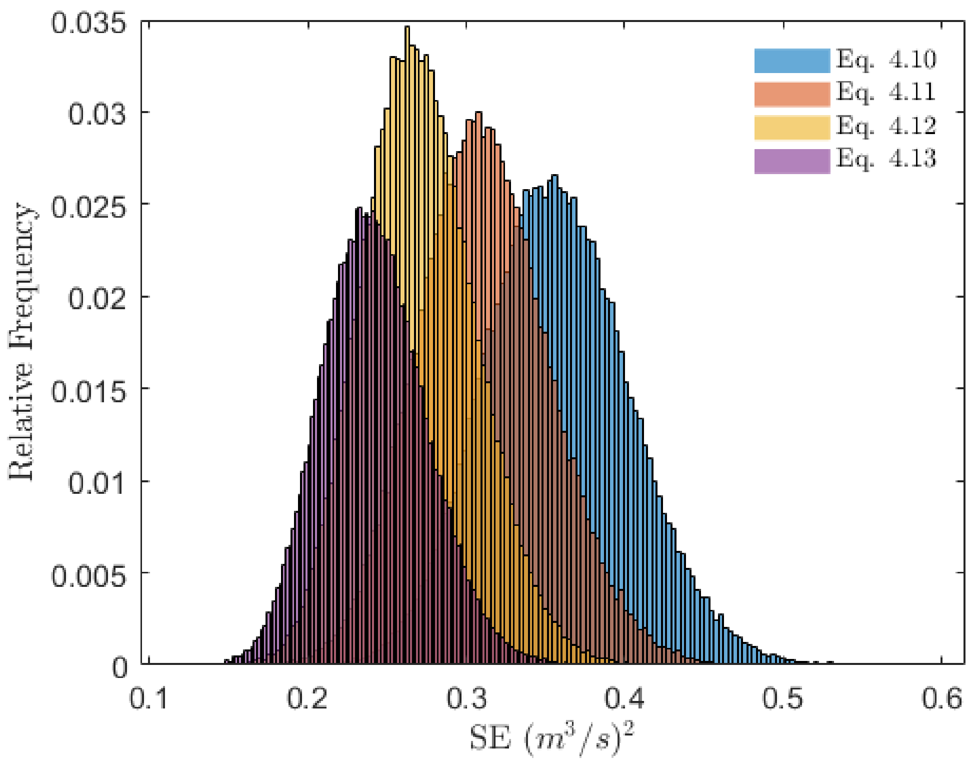

Figure 4.11: Relative frequency distribution of squared error (SE) by bootstrap sampling with N = 100,000.

Table 4.2: Summary of error statistics for the four alternative stage-discharge equations for Obermeyer pivot weirs.

	MAPE(%)	MSE	95% C.I.
Eq. (4.10)	9.0	0.36	(0.27,0.45)
Eq. (4.11)	8.3	0.31	(0.23,0.40)
Eq. (4.12)	7.8	0.27	(0.20,0.34)
Eq. (4.13)	7.4	0.24	(0.18,0.31)

4.4.1 Significance of results

The results presented in Figure 4.11 and Table 4.2 reveal the expected outcome that the accuracy of the rating equation increases with complexity related to a reliance upon empirical calibration and auxiliary measurement. The MSE of each respective approach was found to be significantly different from the MSE of every other approach at a significance level of $p < 0.05$. The best performing rating equation was (4.13), which requires knowledge of both the inclination angle and the upstream velocity head. The worst performing equation was (4.10), which neglects the effect of both the inclination angle and the velocity head on the rating equation. The interesting result seen here is that Eq. (4.12), the approach requiring empirical calibration of the inclination angle effect, performed significantly better than Eq. (4.11), which has a more theoretical foundation that makes it potentially generalizable to pivot weirs of varying geometric characteristics. Thus, the hypothesis laid out in Section 4.1 that the effect of the gate angle on the flow dynamics could be completely accounted for by taking into account the total upstream mechanical energy head, rather than solely the upstream elevation head, proved false. This hypothesis relied on the assumption that viscous effects could be sufficiently ignored between the upstream stage measurement location and the crest, even as the inclination angle of the gate was altered. Evidently, some secondary process is at work within the flow dynamics such that the relative magnitude of the viscous force experienced by the flow also happens to be a function of the inclination angle. In other words, the relationship between the inclination angle and the velocity head of the flow is non-linear, so that simply incorporating H into the rating equation is insufficient to account for the effect of altering θ. Evidence for this conclusion is found in Figure 4.1, which reveals the relationship is likely monotonic, but represents a power law rather than a linear relationship. This finding is also supported in part by Eq. (2.18) - the $C_{d_{\theta-h}}$ fit provided by Bijankhan and Ferro (2018). This function predicts that above approximately 45°, the effect of the gate angle becomes nominal. Additionally, recent CFD results produced within the Environmental Fluid Mechanics Laboratory at CSU suggest that $C_{d_{\theta-h}}$ may even increase slightly as $\theta \rightarrow 90°$. For this reason, an empirical calibration for the effect of the changing inclination angle for a pivot weir results in a more accurate rating equation over the theoretical approach of (4.11).

These results also suggest some practical take-aways concerning which additional measurement apparatus should be installed first for accurate pivot weir operation. Imagine a canal manager who operates a pivot weir but currently is only able to measure the water surface elevation upstream of the weir as an input to the stage-discharge equation for flow quantification. These results of the current study suggest that, given the choice, this canal manager should first invest in a means to estimate the inclination angle of the pivot weir under operating circumstances, rather than a way to accurately compute the velocity head of the flow. This would allow them to use (4.12) within an estimated range of accuracy of $\pm 7.8\%$. However, this approach neglects that fact that the discharge coefficient will likely increase with rising values of h/p, due to the large contribution of the velocity head to H at lower gate angles. Therefore, if this canal manager is given the option, they should also consider investing in a means to dynamically estimate the velocity head of the flow at the upstream location, as this will indeed promise even further accuracy in prediction of discharge by the pivot weir.

4.4.2 Comparison with other studies

The optimal approach for establishing a rating equation for an Obermeyer pivot weir has been discussed, along with the effect of the inclination on the flow dynamics over a pivot weir. We now compare the findings of the current study to those from previous studies. The seminal work of Wahlin and Replogle (1994), and the follow-up work of Bijankhan and Ferro (2018) primarily used laboratory pivot weir models, in contrast to the current study which is based entirely on field observations. Earlier studies were also done on a generalized pivot weir, where the leaf gate is flat, in contrast to the cambered gate of the Obermeyer pivot weir. Due to the empirical nature of calibrating hydraulic structures, it remains an open question as to whether a generalized formula can be established that provides an accurate representation of the discharge coefficient and its relationship to gate angle, θ for pivot weirs of similar geometry. First, we examine conclusions from the literature and the current study concerning the general trend of how θ affects C_{d_θ}. The magnitude of, C_{d_θ} is compared for the example of $\theta = 30°$ and $h/p = 0.8$ in Table 4.3 between an approach taken in the current study and those in the earlier literature. The approach examined with respect to the current study is Eq. (4.12), which is the alternative most similar to those found in previous works. The third column in this table reveals a marked difference in the magnitude of C_{d_θ} for the Obermeyer pivot weir examined in the current study, compared to the similar values from previous studies.

Table 4.3: Comparison of discharge coefficient values for a sample case of $\theta = 30°$ and $h/p = 0.8$. C_{d_θ} for Eq. (2.11) is taken as the product of $C_e \cdot C_a$.

Pivot Weir Rating Approach	C_{d_θ}	% diff from Eq. (2.11)
Eq. (2.11) - Wahlin & Replogle (1994)	0.734	
Eq. (2.16) - Bijankhan and Ferro (2018)	0.760	3.64%
Eq. (4.12)	0.625	-14.77%

Due to the empirical nature of the rating equation C_{d_θ}, it is not a simple matter to determine the exact reason for discrepancy between the primarily laboratory-based studies of previous authors, and the field observations of the current study. However, two main hypothesis were formulated in an attempt to explain.

- **Inadequate nappe aeration in laboratory calibration**: One potential reason for the difference in the magnitude of C_{d_θ} between the laboratory and field studies is the difficulty of maintaining sufficient ventilation of the overflowing nappe in the laboratory. The majority of laboratory studies are completed in rectangular flumes which severely constrict the downstream condition of the flow. In the field, there is a divergence of retaining side walls supporting the structure (see Figure 4.2). This separation of the flow from the supporting side wall allows air to flow underneath the nappe and sustain a condition of atmospheric pressure. Wahlin and Replogle (1994) examined data from both laboratory and field measurement campaigns. They observed an over-prediction of Q in the field using a rating equation developed from laboratory data [20]. The structures in the field had a well-ventilated nappe that was allowed to circulate freely downstream of the crest. In the discussion, Wahlin and Replogle (1994) state that difficulty was experienced in the laboratory with preserving a fully supported nappe. Furthermore, Bijankhan and Ferro (2018) make no mention of considerations given to ensuring sufficient nappe aeration, even when their study was performed in a confined flume, which typically limits air ventilation underneath the nappe. The condition of fully atmospheric pressure underneath the nappe for sharp-crested weir flow is a fundamental assumption of the classical rating equation (2.10). Because the rating equation for the pivot weir is derived from this equation, the same assumptions and conditions for proper measurement must apply. Insufficient nappe aeration would allow a higher Q to pass over the structure for a given head (i.e. h/p) than for a fully-aerated structure, thus effectively increasing the discharge coefficient.

- **Boundary layer separation due to camber on Obermeyer gate leaf**: A unique aspect of the pivot weirs examined in this study was the camber incorporated into the gate leaf design. After review of patent reports for the Obermeyer gate, it is not clear to the author why this design choice was made. The camber may provide additional structural integrity to the gate by resisting bending motion under large flows. Additionally, the camber of the gate allows it to better conform to the supporting air bladders and may facilitate more efficient adjustments of the gate inclination angle. Another potential side effect of the cambered Obermeyer gate is separation of the boundary layer flow near the crest. Especially at higher gate angles, the velocity of the flow near the crest is primarily in the vertical direction. As the flow adjacent to the gate leaf passes along the structure, the crest begins to curve away from the tangential direction of the flow. The boundary layer of the flow eventually breaks away from the gate leaf due to the viscous friction of the gate structure near the crest. This phenomena would effectively result in higher energy losses as the flow passes over the crest, and necessitate a higher upstream head to pass a given Q over the crest. Thereby, the camber along the Obermeyer gate would essentially reduce the magnitude of C_d.

4.5 Laboratory Pivot Weir Model

To investigate the above hypotheses, preliminary tests were conducted in the Environmental Fluid Mechanics Laboratory at Colorado State University during Spring 2021. A laboratory model of the Gate A Obermeyer pivot weir was constructed using primarily acrylic, stainless steel, and a rubber piano hinge (see Figure 4.12). The width of the model is $b = 30cm$ and the gate length is $L_g = 7cm$ This ratio of $L_g/b =\sim 0.25$ was consistent with the aspect ratio of the Gate A Obermeyer pivot weir observed in the field. The exact curvature for the camber the gate was not available from structural drawings of the Obermeyer pivot weir, due to the proprietary nature of the device. Therefore, the geometry was estimated by the author to produce the camber of the lab model gate using rolled stainless steel with a radius of curvature of 167 mm. The lab model has a angular range of $22° \leq \theta \leq 90°$ by 5 degree increments. Hence, there are 15 possible gate angles that can be examined using the gate. Partial aeration of the nappe is provided by a structural support piece that secures the angle of the gate and protrudes slightly into the overflowing nappe. Further enhancement to ensure full aeration of the nappe is planned.

4.5.1 Laboratory Methodology

Preliminary observations of flow over the model Obermeyer pivot weir were completed using Particle Image Velocimetry (PIV). This methodology involves capturing high speed images of flow containing 20 μm diameter seeding particles. These particles are illuminated by a dual cavity laser connected to a high speed camera. This camera is able to capture between 200-800 images per second, which are then concatenated in a series to form a movie. The result is a richly resolved

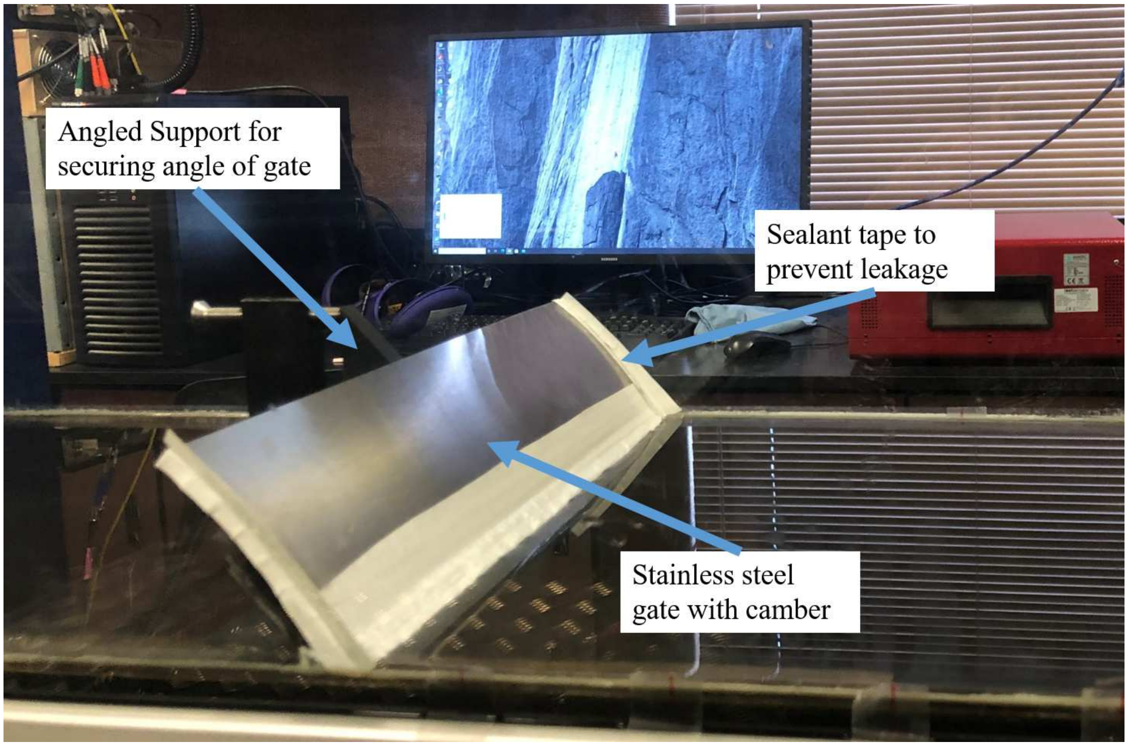

Figure 4.12: Laboratory model of an Obermeyer pivot weir at the Environmental Fluid Mechanics Laboratory - Colorado State University.

two-dimensional picture of the flow velocity field, making computation of insightful second order statistics possible. All post-processing of PIV images was completed using DaVis 10 software, while data analysis of exported PIV data was completed in MATLAB (v. 2020a).

Measurements of upstream water depth were made using a mobile point gauge with a Vernier scale accurate to 0.001ft. Flow rate was determined using an electromagnetic flowmeter accurate to $\pm 1\%$, and was also compared to Q calculated using the depth-averaged velocity of the flow calculated using the PIV. Percent difference between values of Q determined using the PIV and the electromagnetic flowmeter did not exceed 5%.

4.5.2 Initial Findings

Preliminary investigations focused on qualitative observations of flow structure for the Obermeyer pivot weir model set vertically ($\theta = 90°$). Figure 4.13 reveals several interesting qualitative observations of the flow field. Firstly, evidence for boundary layer separation is found near the

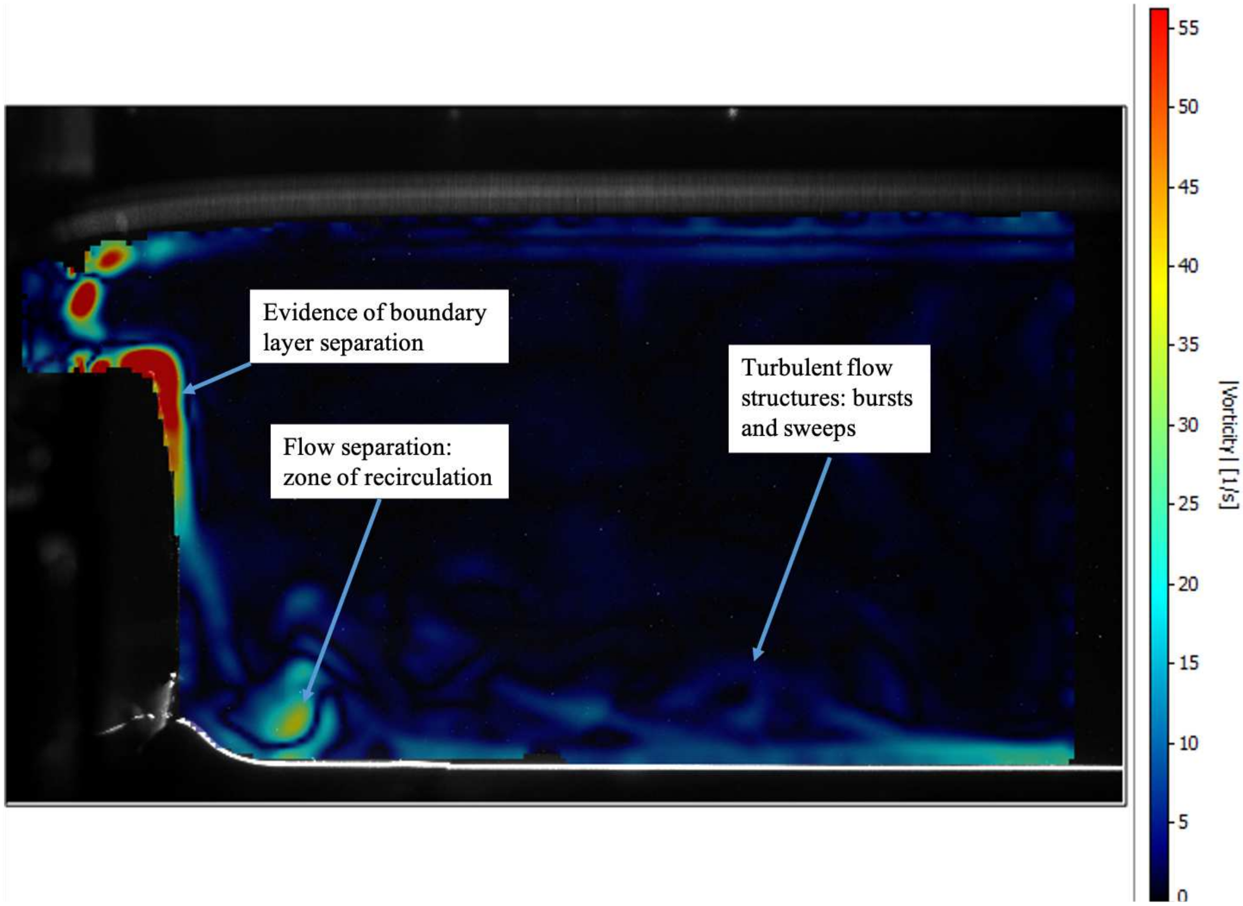

Figure 4.13: Post-processed PIV image of flow over laboratory model of Obermeyer pivot weir set at 90°. $Q = 2.41(L/s)$ and $h/p = 0.43$. Color scale on right hand side represents measurement of vorticity in revolutions/second.

crest. By definition, turbulent flow is highly rotational and hence has non-zero vorticity [60]. As the boundary layer separates, the flow becomes especially turbulent and exhibits violent vortical motions [9]. Kinetic energy is dissipated in this region due to the transfer of fluid inertia into diffusive heat due to viscosity. The high amount of vorticity ($\omega = \nabla \times \mathbf{U}$) shown in Figure 4.13 as the flow navigates the gate leaf and passes over the crest is potential evidence that the camber in the Obermeyer gate design leads to boundary layer separation near the crest and additional dissipative kinetic energy losses. However, further experimentation is needed to examine the flow structure in the vicinity of the crest for different gate leaf geometries to determine anything conclusive.

Some additional calibration data for $C_{d_{\theta-h}}$ were gathered using the laboratory Obermeyer pivot weir for $\theta = 90°$. A similar procedure as described in Section 4.3 was used for six measurements ranging from $0.3 \leq h/p \leq 1.0$ and $1.22 \leq Q(L/s) \leq 11.22$. The estimated value of $C_{d_{\theta-h}}$ for $\theta = 90°$ was 0.60 using the lab model. This represented an approximately 11% increase in the value of 0.535 for the lower limit of $C_{d_{\theta-h}}$ that was expected from (4.7). However, Bijankhan and Ferro (2018) hypothesized that above a certain value of θ, the effect of the angle of the gate on the nature of the flow becomes nominal. Additionally, as discussed in Section 4.4.1, $C_{d_{\theta-h}}$ may even increase as $\theta \rightarrow 90°$. However, these results are so far inconclusive and require further validation.

Table 4.3 shows that the general magnitude for $C_{d_{\theta-h}}$ of the field data collected in the current study was significantly different than the values from by previous studies. Although the magnitude of $C_{d_{\theta-h}}$ in the current study differs from that of previous studies, it is possible to compare the relative trend of C_{d_θ} vs. θ between studies presented in the literature. Wahlin and Replogle (1994) listed a discharge ratio specific to the gate angle, known as the flow amplification factor, or Q/Q_{90} - Eq. (2.15). This value represents the ratio of the flow that is able to pass over a pivot weir with a given head for a given value of θ, compared to the flow over the classic vertical sharp-crested weir with that same upstream head. An intriguing aspect of a pivot weir is that it allows for the conveyance of a greater Q compared to a sharp-crested weir operating at the same upstream stage level, while also maintaining regulation over the water level. However, the use of a pivot also increase the magnitude of the flow velocity near the structure, necessitating the consideration of canal bed scouring. For rating equations that are not dependent on h/p, the flow amplification factor is simply:

$$\frac{Q_\theta}{Q_{90°}} = \frac{C_{d_\theta}}{C_{d_{90°}}}. \tag{4.16}$$

If the lower limit of the field-scale Obermeyer pivot weir $C_{d_{\theta-h}}$ is taken to be the value recently calibrated using laboratory experiments, then Eq. (4.7) can be normalized by $C_{d_{90°}} = 0.600$. If these relative discharge coefficient values are then fit to a curve using non-linear regression as a function of $\theta(rad)$, the general trend of $C_{d_{\theta-h}}$ vs. θ from approach 3 within the present study can be written as:

$$\frac{Q_\theta}{Q_{90°}} = 0.913(\theta)^{-0.207}; \tag{4.17}$$

where θ is given in radians, and is valid for $0.358 \leq \theta(rad) \leq 0.634$. This trend can be compared to the findings of Wahlin and Replogle (1994) and Bijankhan and Ferro (2018), respectively [20, 22].

Analysis of Figure 4.14 reveals major discrepancy regarding the nature of the mathematical relationship between $C_{d_{\theta-h}}$ and θ. Data related to Bijankhan and Ferro (2018) and the current

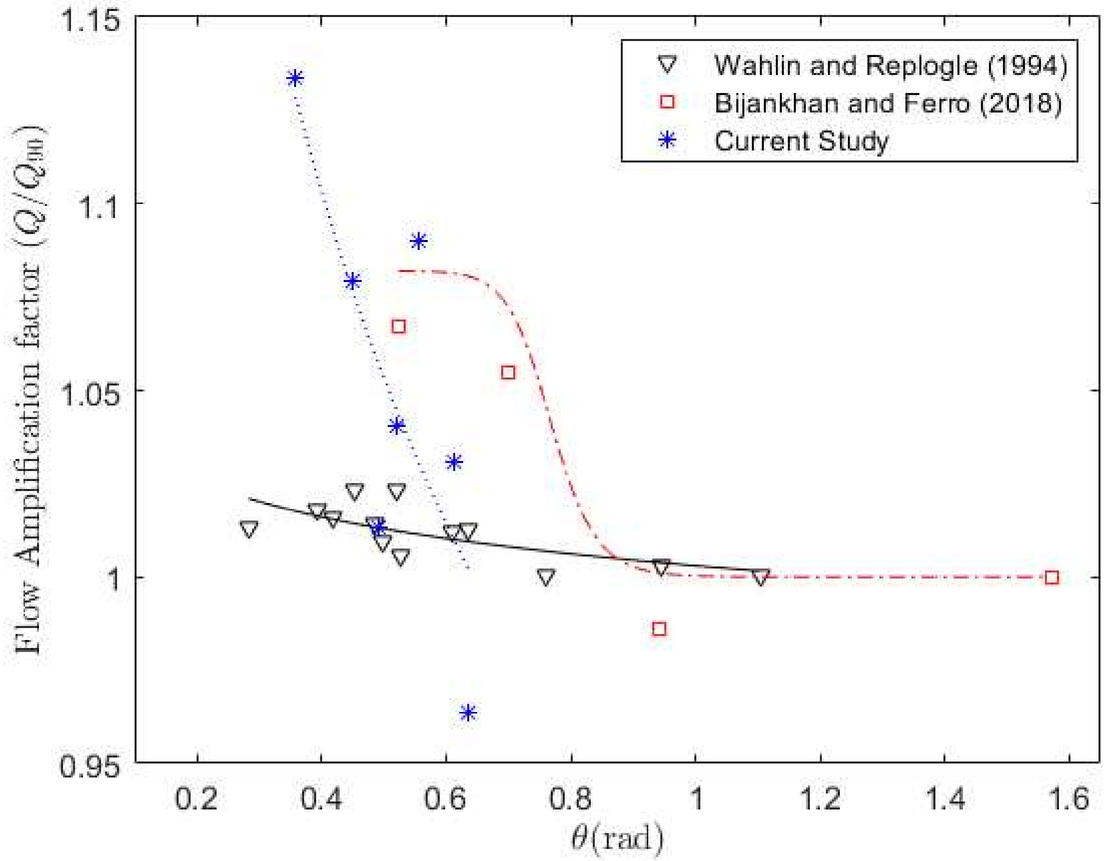

Figure 4.14: The effect of gate angle on flow amplification factor, as found by three distinct studies. Raw data used for calibration shown, as well as best fit curved found as a result of least squares regression.

study match fairly well, exhibiting a significant effect of θ on the flow ratio from approximately $0.4(23°) \leq \theta \leq 0.79(45°)$. The effect of θ on $Q/Q_{90°}$ for the Wahlin and Replogle (1994) seems to be of a smaller magnitude, suggesting a possible dependency of $Q/Q_{90°}$ on specific structure design parameters. The variability of $Q/Q_{90°}$ within this range thus justifies further experimental investigation. Interestingly, both previous studies suggest the effect of θ on the flow dynamics for the pivot weir are nominal beyond $\theta = 0.79(45°)$. This is contrast to the initial hypothesis of the current study described in Section 4.1, but is consistent with the results of the error analysis for the alternative rating equation approaches given in Section 4.4.

4.6 Summary of Field and Laboratory Findings

In light of the observations examined in the chapter, the following conclusions can be made:

- The optimal approach for establishing a rating equation for the Obermeyer pivot weir involves empirical calibration to account for the effect of the changing inclination angle on the flow dynamics. A simplified theoretical approach which assumes this effect can be completely resolved by consideration of the total mechanical energy head within the rating equation, performed worse in comparison to the approach reliant upon empirical calibration.

- Necessity for empirical calibration of hydraulic structures to achieve accurate flow quantification provides further motivation for the work presented in Chapter 3. Calibration of hydraulic structures can principally be achieved using velocity-area methods, of which the ADCP is the most widely-used, being both time-efficient and fairly accurate.

- When available, accounting for the effect of the velocity head on the upstream energy condition of the flow results in a significant improvement in the accuracy of the rating equation. This is because the relative contribution of the velocity head to the overall total mechanical energy head increases as θ decreases.

- The effect of θ on the relative distribution of potential and kinetic energy within the flow has been elucidated by the current study but remains yet to be fully understood. Comparisons between the current study and previous literature show a significant effect from approximately $23° \leq \theta \leq 45°$, with nominal effects beyond $\theta = 45°$. Furthermore, the magnitude of the flow amplification effect due to the inclination angle has not been resolved within the literature and requires further investigation.

- The magnitude of the discharge coefficient for the Obermeyer pivot weir operating within the field was markedly lower than what other authors have predicted based upon laboratory data. Hence, interacting factors of poor nappe ventilation for laboratory calibrations, and boundary layer separation due to the camber of the Obermeyer gate may decrease the discharge coefficient pivot weir Obermeyer structure by 15%.

Chapter 5

Summary and Conclusions

5.1 Summary of Investigation

This thesis addresses methods and principles for accurately quantifying flow rate in irrigation canals, with a focus on the reduction in measurement uncertainty and enhancement of the empirical calibration of stage-discharge relationships for hydraulic structures.

Chapter 1 opened with background information on the basic task of open-channel flow quantification and the often overlooked cascading consequences to water management. Chapter 2 gave a review of relevant literature and basic knowledge on the subjects of flow measurement in open-channels, as well as stage-discharge equations used for rating hydraulic structures.

Chapter 3 detailed an extensive field measurement campaign across four different irrigation canal measurement sites in Northern Colorado. Refinement of current best practice guidelines was pursued to improve the clarity and accuracy of discharge measurement procedures for ADCPs. User specific protocols were targeted for improvement since these are the most readily adapted and simple to analyze guidelines.

Chapter 4 investigated several alternative approaches for developing a stage-discharge rating equation for an Obermeyer pivot weir. Special consideration was given to the nature of the discharge coefficient and how it relates to the changing angle of the gate. A hypothesis concerning an aspect of the theoretical foundation for the pivot weir rating equation was also investigated. Field observations presented in this chapter represent a novel contribution to the literature and highlight the empirical nature of discharge coefficient values. Preliminary findings from experimentation with a laboratory model of the Obermeyer pivot weir offer intriguing insights into flow dynamics around hydraulic structures.

5.2 Major Conclusions

- Maintenance of a steady boat speed when conducting ADCP moving-boat discharge measurements is of critical importance to ensuring accurate data collection. For this purpose, investment in a remotely-operated tagline deployment system is recommended over using a manual rope-and-pulley system.

- Previous guidelines concerning ADCP measurement protocols suggested a total measurement duration of 720 s taken over a minimum of two transects. These guidelines were seen by the author as being too ambiguous for accurate discharge measurement because they suggest the ADCP moving-boat should travel at drastically different speeds dependent on the size of the canal. For small canals, this risks prescribing an unrealistically small value for the speed of the moving-boat that reduces measurement time efficiency and compromises the steady motion of the boat. For large canals, these guidelines risk moving the boat too fast, so that the full fluctuating turbulent velocity field is not fully observed and a temporally-biased computation of the mean discharge is made.

- Refinement of user protocols for ADCP discharge measurements beyond previously ambiguous guidelines resulted in recommendations for a per-transect duration, made relative to the approximate top-width of the canal, of 24 s/m (7.3 s/ft) for an ADCP measuring in small to midsize irrigation canals at a frequency of 1 Hz. This rate of data collection aims to resolve the fluctuating velocity field of the turbulent flow and obtain a more accurate measurement of mean discharge. A minimum of six transects are recommended for computation of mean steady discharge as a point of optimal return for collecting a sufficiently large amount of data while performing the measurement in a time-efficient manner.

- A reduction between 30-70% in the uncertainty of discharge measurement made using an ADCP was observed when following the previously listed refined protocols. This allows for more accurate flow measurement using an ADCP, as well as for more accurate calibration of hydraulic structures.

- The idea that uncertainty in ADCP discharge measurements is a non-issue, due to deviations in individual discharge observations from a mean value eventually having a cumulative zero-effect under a sufficiently large sample size, was refuted. ADCP discharge measurements are not achieved within large sample sizes, as evidenced by Chapter 3 where N_t is recommened to be only six. Hence, the pursuit of reducing the uncertainty in an ADCP discharge measurement around the true mean value is worthwhile.

- An error analysis of four alternative approaches for developing a rating equation for the Obermeyer pivot weir revealed that the most accuracy in predicting discharge is achieved when an empirically-derived coefficient is introduced that is a function of the gate inclination angle. Further accuracy can also be gained if the contribution of the velocity head to the rating equation is considered.

- The effect of the inclination angle on the flow dynamics of pivot weirs is not a trivial phenomenon. A hypothesis that built upon the inviscid flow assumption to postulate that altering the inclination angle of the pivot weir simply redistributes the relative amount of elevation head and velocity head within the flow was proven wrong. Thus, a secondary mechanism, likely tied to the dynamic nature of the viscous effects experienced by the flow, was identified as a topic for further investigation.

- Analysis of field data presented in this thesis revealed that the magnitude of the discharge coefficient for the Obermeyer pivot weir was about 15% less than that estimated by previous authors for a flat-plate inclined sharp-crested weir. Hypotheses concerning the insufficiency of nappe aeration within laboratory studies and boundary layer separation due to the camber design of Obermeyer gate leaf were discussed as potential explanations for the difference.

- When the effect of the gate angle is normalized by the discharge coefficient for a sharp-crested vertical weir, some inconclusive trends in the literature are revealed concerning the nature of the mathematical relationship between the gate angle and the discharge capacity of the structure.

- Elucidation on the nature of the flow dynamics for an Obermeyer pivot weir and proposal of four alternative rating equation approaches for use with this structure lays the groundwork for the development and application of a generalized rating relationship for structures of a similar type. This novel development for the rating of pivot weirs as both a stage management and flow measurement structure represents an especially important contribution to the goal of efficient and equitable irrigation water management.

5.3 Directions for Future Research

The applicability of the findings presented in Chapter 3 to larger open-channels with more natural aspect ratios is an element of future study. An ADCP is a widely-used instrument for a multitude of applications that require accurate flow measurement. Additionally, revisiting these established protocols when more robust ADCPs with higher sampling frequencies are available on the market would inform the scalability of the present findings. Preliminary studies concerning measurement with higher frequency ADVs and the turbulent statistics of natural flows could be one avenue of approach.

The most accessible direction for future research will be to continue with preliminary investigations of the laboratory model Obermeyer pivot weir and to examine whether or not initial findings from the field data set support initial findings. A comprehensive parametric study on the effect of gate angle on the discharge coefficient for a pivot weir rating equation is attainable with current laboratory equipment, and will be greatly enhanced by the explanatory and visualization power of PIV data analysis. Specific interest will be placed on investigating the validity of the fundamental assumptions implicit in the pivot weir rating equation and identifying practical methods for mitigating the effect of inaccuracy in flow quantification that occurs when these assumptions are violated.

Furthermore, opportunity for investigating the parameterization of rating equations for other hydraulic structures, such as the Parshall flume and sluice gates, may also be a direction for future investigations. The goal will be two-fold: to pursue novel insights concerning the nature of flow quantification using hydraulic structures via emergent experimental and computational fluid dynamics techniques; and the full consideration of practical implementation constraints faced by irrigation water managers, necessitating clear and concise communication to identify optimal approaches.

Bibliography

[1] R Wade and R Chambers. Managing the Main System: Canal Irrigation's Blind Spot. *Economic and Political Weekly*, 19(30):A107 – A112, 1980.

[2] Interagency Task Force. Irrigation water use and management. *US Government Printing Office*, 1979.

[3] David J. Molden and Timothy K. Gates. Performance Measures for Evaluation of Irrigation-Water-Delivery Systems. *Journal of Irrigation and Drainage Engineering*, 116(6):804–823, 11 1990.

[4] Pieter R. Van Oel, Maarten S. Krol, and Arjen Y. Hoekstra. A river basin as a common-pool resource: A case study for the Jaguaribe basin in the semi-arid Northeast of Brazil. *International Journal of River Basin Management*, 7(4):345–353, 2009.

[5] Hilary McMillan, Jan Seibert, Asgeir Petersen-Overleir, Michel Lang, Paul White, Ton Snelder, Kit Rutherford, Tobias Krueger, Robert Mason, and Julie Kiang. How uncertainty analysis of streamflow data can reduce costs and promote robust decisions in water management applications. *Water Resources Research*, 53(7):5220–5228, 7 2017.

[6] Linda O. Mearns, Cynthia Rosenzweig, and Richard Goldberg. Mean and variance change in climate scenarios: Methods, agricultural applications, and measures of uncertainty. *Climatic Change*, 35(4):367–396, 1997.

[7] A.A. Rehman Lund, Chad A. Martin, Timothy K. Gates, Joseph Scalia, and M. Munir Babar. Field evaluation of a polymer sealant for canal seepage reduction. *Agricultural Water Management*, 252:106898, 6 2021.

[8] D.W. Spitzer, editor. *Flow measurement: practical guides for measurement and control*. The Instrumentation, Systems, and Automation Society, 2nd edition, 2001.

[9] Pijush K Kundu, Ira M Cohen, and David R. Dowling. *Fluid Mechanics*. Elsevier, 6th edition, 2016.

[10] R W Herschy. *Streamflow Measurement*. Taylor & Francis, New York, 3rd edition, 2009.

[11] David S Mueller, C Russell Wagner, Michael S Rehmel, Kevin A Oberg, and Francois Rainville. *Measuring discharge with acoustic Doppler current profilers from a moving boat*. US Department of the Interior, US Geological Survey Reston, Virginia (EUA), 2.0 edition, 2013.

[12] Subhash C Jain. *Open-channel flow*. John Wiley & Sons, 2001.

[13] M G Bos. DISCHARGE MEASUREMENT STRUCTURES Working Group on Small Hydraulic Structures. Technical report, Working Group on Small Hydraulic Structures, 1976.

[14] Henry K. Obermeyer. Water control apparatus, 2013.

[15] A. Malcherek. 300 Years 'De motu aquae mixto': What Poleni really wrote and a new overflow theory based on momentum balance. *7th IAHR International Symposium on Hydraulic Structures, ISHS 2018*, pages 78–88, 2018.

[16] F.M. Henderson. *Open Channel Flow*. Macmillan Publishing Co., Inc, New York, 1966.

[17] Michael C. Johnson. Discharge coefficient analysis for flat-topped and sharp-crested weirs. *Irrigation Science*, 19(3):133–137, 2000.

[18] M. Bijankhan, C. Di Stefano, and V. Ferro. Generalised stage–discharge relationship for rectangular weirs. *Proceedings of the Institution of Civil Engineers: Water Management*, 171(3):125–133, 2018.

[19] Carl E. Kindsvater and Rolland W. Carter. Discharge Characteristics of Rectangular Thin-Plate Weirs. *Transactions of the American Society of Civil Engineers*, 124(1):772–801, 1 1959.

[20] B T Wahlin and J A Replogle. Flow Measurement Using An Overshot Gate. Technical report, United States Bureau of Reclamation, 1994.

[21] Joseph M Sinclair, Subhas Karan Venayagamoorthy, and Timothy K. Gates. Working Paper: Some Insight on Flow over Sharp-crested Weirs using Computational Fluid Dynamics. *Journal of Irrigation and Drainage Engineering*, 2021.

[22] Mohammad Bijankhan and Vito Ferro. Experimental Study and Numerical Simulation of Inclined Rectangular Weirs. *Journal of Irrigation and Drainage Engineering*, 144(7):04018012, 7 2018.

[23] A. S. Hamilton and R. D. Moore. Quantifying uncertainty in streamflow records. *Canadian Water Resources Journal*, 37(1):3–21, 2012.

[24] Marian Muste, Dennis A Lyn, David Admiraal, Robert Ettema, Vladimir Nikora, and Marcelo H Garcia. *Experimental Hydraulics: Methods, Instrumentation, Data Processing and Management: Volume I: Fundamentals and Methods*. CRC Press, 2017.

[25] S J Kline. The purposes of uncertainty analysis. *Journal of Fluids Engineering*, 107, 1985.

[26] United Nations (UN). Back to Our Common Future. Technical report, United Nations, 2012.

[27] N Mancosu, R L Snyder, G Kyriakakis, and D Spano. Water scarcity and future challenges for food production. Water 7: 975-992. *Water*, 7:975–992, 2015.

[28] S. E. Rantz. *Measurement and computation of streamflow: volume 1. Measurement of stage and discharge.* U.S. Dept. Interior, 1981.

[29] Jochen Aberle, Colin Rennie, David Admiraal, and Marian Muste. *Experimental Hydraulics: Methods, Instrumentation, Data Processing and Management: Volume II: Instrumentation and Measurement Techniques*. CRC Press, 2017.

[30] P. A. Carling, H. Trieu, D. D. Hornby, He Qing Huang, S. E. Darby, D. A. Sear, C. Hutton, C. Hill, Z. Ali, A. Ahmed, I. Iqbal, and Z. Hussain. Are equilibrium multichannel networks

predictable? The case of the regulated Indus River, Pakistan. *Geomorphology*, 302:20–34, 2018.

[31] Jose Cândido Stevaux, Hudson de Azevedo Macedo, Mario Luis Assine, and Aguinaldo Silva. Changing fluvial styles and backwater flooding along the Upper Paraguay River plains in the Brazilian Pantanal wetland. *Geomorphology*, 350:106906, 2020.

[32] Amir Mohammadi, Atefeh Parvaresh Rizi, and Nader Abbasi. Field measurement and analysis of water losses at the main and tertiary levels of irrigation canals: Varamin Irrigation Scheme, Iran. *Global Ecology and Conservation*, 18:e00646, 2019.

[33] Juan A González-Castro and Marian Muste. Framework for estimating uncertainty of ADCP measurements from a moving boat by standardized uncertainty analysis. *Journal of Hydraulic Engineering*, 133(12):1390–1410, 2007.

[34] Emily Perrin. On Some Dangers of Extrapolation. *Biometrika*, 3(1):99–103, 1904.

[35] T. Tokyay, G. Constantinescu, and Juan A. Gonzalez-Castro. Investigation of Two Elemental Error Sources in Boat-Mounted Acoustic Doppler Current Profiler Measurements by Large Eddy Simulations. *Journal of Hydraulic Engineering*, 135(11):875–887, 2009.

[36] Marian Muste, Dongsu Kim, and Juan A González-Castro. Near-transducer errors in ADCP measurements: Experimental findings. *Journal of Hydraulic Engineering*, 136(5):275–289, 2010.

[37] Kyutae Lee, Hao Che Ho, Muste Marian, and Chun Hung Wu. Uncertainty in open channel discharge measurements acquired with StreamPro ADCP. *Journal of Hydrology*, 509:101–114, 2014.

[38] International Organization for Standardization. *Uncertainty of Measurement-Part 3: Guide to the Expression of Uncertainty in Measurement (GUM: 1995)*. ISO, 2008.

[39] M. Cox, P. Harris, and B. R.L. Siebert. Evaluation of measurement uncertainty based on the propagation of distributions using Monte Carlo simulation. *Measurement Techniques*, 46(9):824–833, 2003.

[40] R W Herschy. Estimation of uncertainties in hydrometric measurements. In *Critical Transitions in Water and Environmental Resources Management*, pages 1–9. ASCE, 2004.

[41] R. Daren Harmel and Patricia K. Smith. Consideration of measurement uncertainty in the evaluation of goodness-of-fit in hydrologic and water quality modeling. *Journal of Hydrology*, 337(3-4):326–336, 4 2007.

[42] David S Mueller. QRev - Software for Computation and Quality Assurance of Acoustic Doppler Current Profiler Moving-Boat Streamflow Measurements - User's Manual for Version 2.8. Technical Report March, USGS, 2016.

[43] Hening Huang. Estimating Bias Limit of Moving-Boat ADCP Streamflow Measurements. *Journal of Hydraulic Engineering*, 144(6):04018024, 2018.

[44] J. Le Coz, B. Blanquart, K. Pobanz, G. Dramais, G. Pierrefeu, A. Hauet, and A. Despax. Estimating the Uncertainty of Streamgauging Techniques Using In Situ Collaborative Interlaboratory Experiments. *Journal of Hydraulic Engineering*, 142(7):04016011, 2016.

[45] A Despax, J Le Coz, A Hauet, F L Engel, K A Oberg, G Dramais, D Besson, and A Belleville. Quantifying the site selection effect in the uncertainty of moving-boat ADCP discharge measurements. *HMEM*, NA(July):8, 2018.

[46] Aurélien Despax, Jérôme Le Coz, Alexandre Hauet, David S. Mueller, Frank L. Engel, Bertrand Blanquart, Benjamin Renard, and Kevin A. Oberg. Decomposition of Uncertainty Sources in Acoustic Doppler Current Profiler Streamflow Measurements Using Repeated Measures Experiments. *Water Resources Research*, 55(9):7520–7540, 2019.

[47] Matthew R. Klema, Abdul G. Pirzado, S. Karan Venayagamoorthy, and Timothy K. Gates. Analysis of acoustic Doppler current profiler mean velocity measurements in shallow flows. *Flow Measurement and Instrumentation*, 74(June), 2020.

[48] Carlos M. García, Leticia Tarrab, Kevin Oberg, Ricardo Szupiany, and Mariano I. Cantero. Variance of Discharge Estimates Sampled Using Acoustic Doppler Current Profilers from Moving Platforms. *Journal of Hydraulic Engineering*, 138(8):684–694, 2012.

[49] Kevin Oberg and David S Mueller. Validation of streamflow measurements made with acoustic Doppler current profilers. *Journal of Hydraulic Engineering*, 133(12):1421–1432, 2007.

[50] Brandy Armstrong. Best Practices Caring for Acoustic Instruments.

[51] Teledyne RDI. StreamPro ADCP Operation Manual. Technical Report February, Teledyne RD Instruments, 2004.

[52] Hening Huang. Estimating uncertainty of streamflow measurements with moving-boat acoustic Doppler current profilers. *Hydrological Sciences Journal*, 63(3):353–368, 2018.

[53] James W. Eckblad. Biologist's Toolbox: How many samples should be taken ? *BioScience*, 41(5):346–348, 1991.

[54] Paul H. Kvam and Brani Vidakovic. *Nonparametric Statistics with Applications to Science and Engineering*. John Wiley & Sons, Hoboken, NJ, 2007.

[55] Andy Pineda P.E. Personal Communication with Andy Pindea. Technical report, Larimer and Weld Irrigation, Fort Collins, CO, 2020.

[56] Michael R. Simpson. Discharge Measurements using a broad-band acoustic Doppler current profiler. Technical report, USGS, 2001.

[57] Caner Kutlu. Calibration and uncertainty of a head-discharge relationship for overshot gates under field conditions, 2019.

[58] Joseph E. Pugh, Timothy K. Gates, and S. Karan Venayagamoorthy. Working Paper: Refining protocols to mitigate user-induced uncertainty in ADCP moving-boat discharge measurements in irrigation canals. *Flow Measurement and Instrumentation*, 2021.

[59] Thomas Diciccio and Robert Tibshirani. Bootstrap confidence intervals and bootstrap approximations. *Journal of the American Statistical Association*, 82(397):163–170, 1987.

[60] Stephen B Pope. *Turbulent flows*. Cambridge University Press, 2001.